

# **DESIGN AND EXPERIMENTAL IMPLEMENTATION OF VARIOUS CONTROLLERS FOR TWIN ROTOR MIMO SYSTEM**

A DISSERTATION

SUBMITTED IN PARTIAL FULFILLMENT OF THE REQUIREMENTS  
FOR THE AWARD OF THE DEGREE  
OF

MASTER OF TECHNOLOGY  
IN  
CONTROL AND INSTRUMENTATION

Submitted by:

**AYUSH**

**2K17/C&I/05**

Under the supervision of

**DR. SUDARSHAN K VALLURU**  
(ASSOCIATE PROFESSOR)



**DEPARTMENT OF ELECTRICAL ENGINEERING**  
**DELHI TECHNOLOGICAL UNIVERSITY**

(Formerly Delhi College of Engineering)  
Bawana Road, Delhi-110042

**DEPARTMENT OF ELECTRICAL ENGINEERING**  
**DELHI TECHNOLOGICAL UNIVERSITY**  
(Formerly Delhi College of Engineering)  
Bawana Road, Delhi-110042

**CANDIDATE'S DECLARATION**

I, Ayush, Roll No. 2K17/C&I/05 student of M.Tech. (Control and Instrumentation), hereby declare that the project Dissertation titled “ Design and experimental implementation of various controllers for Twin rotor MIMO system” which is submitted by me to the Department of Electrical Engineering Department, Delhi Technological University, Delhi in partial fulfillment of the requirement for the award of the degree of Master of Technology, is original and not copied from any source without proper citation. This work has not previously formed the basis for the award of any Degree, Diploma Associate ship, Fellowship or other similar title or recognition.

Place: Delhi

**(Ayush)**

Date:

**DEPARTMENT OF ELECTRICAL ENGINEERING**  
**DELHI TECHNOLOGICAL UNIVERSITY**

(Formerly Delhi College of Engineering)  
Bawana Road, Delhi-110042

**CERTIFICATE**

I, Ayush, Roll No. 2k17/C&I/05 student of M. Tech. (Control & Instrumentation), hereby declare that the dissertation/project titled “ Design and experimental implementation of various controllers for Twin rotor MIMO system” under the supervision of Associate Prof. Dr. Sudarshan K. Valluru of Electrical Engineering Department Delhi Technological University in partial fulfillment of the requirement for the award of the degree of Master of Technology has not been submitted elsewhere for the award of any Degree.

Place: Delhi

**(Ayush)**

Date:

**(DR. Sudarshan K. Valluru)**  
ASSOCIATE PROFESSOR

**DEPARTMENT OF ELECTRICAL ENGINEERING**  
**DELHI TECHNOLOGICAL UNIVERSITY**  
(Formerly Delhi College of Engineering)  
Bawana Road, Delhi-110042

**ACKNOWLEDGEMENT**

I would like to express my gratitude towards all the people who have contributed their precious time and effort to help me without whom it would not have been possible for me to understand and complete the project.

I would like to thank Associate Prof. Dr. Sudarshan K. Valluru, DTU Delhi, Department of Electrical Engineering, my Project guide, for supporting, motivating and encouraging me throughout the period of this work was carried out. His readiness for consultation at all times, his educative comments, his concern and assistance even with practical things have been invaluable.

Date:

AYUSH  
(2K17/C&I/05)  
M.Tech (Control and Instrumentation)

## CONTENTS

<b>Candidate declaration</b>	<b>ii</b>
<b>Certificate</b>	<b>iii</b>
<b>Acknowledgments</b>	<b>iv</b>
<b>Contents</b>	<b>v</b>
<b>List of Figures</b>	<b>viii</b>
<b>List of Tables</b>	<b>ix</b>
<b>List of Acronyms</b>	<b>x</b>
<b>Abstract</b>	<b>xi</b>
<b>CHAPTER-1</b>	
<b>INTRODUCTION</b>	
1.1 General	1
1.2 Literature Review	1
1.3 Thesis Organization	3
<b>CHAPTER-2</b>	
<b>MODELING OF TRMS</b>	
2.1 TRMS Description	4
2.2 TRMS Mathematical Modeling	6
2.3 TRMS Non-linear Simulation Model	9
2.4 TRMS Model Transfer function	10
2.5 Linearized Model	13
2.6 State space model	16
<b>CHAPTER-3</b>	
<b>CONTROLLER DESIGN</b>	
3.1 Introduction	19
3.2 Proportional Integral Derivative Controller (PID)	20
3.2.1 Integer order Proportional Integral Derivative Controller (IO-PID)	20
3.3 Fractional Order Controller	

3.3.1 Introduction	21
3.3.2 Fractional Calculus	22
3.3.3 Definition of Fractional Calculus	22
3.3.3.1 Grunwald-Letnikov (GL) definition	22
3.3.3.2 Riemann-Liouville (RL) definition	23
3.3.3.3 M. Cauputo definition	23
3.3.4 Fractional Order PID Controller	24
3.3.5 Advantages of Fractional Controller over Conventional PID Controller	26
3.3.6 Disadvantages of FPID	27
3.3.7 Tuning of PID	27
3.3.8 Tuning Methods for Fractional Order Controller	
3.3.8.1 Rule Base methods	28
3.3.8.2 Analytical methods	29
3.3.8.3 Self Tuning and Auto Tuning	29
3.3.9 Classical Tuning Procedure for Fractional Order PID Controller	30

## **CHAPTER-4**

### **CONTROLLER SCHEME USING FOI-PD, FOPID & IO-PID CONTROLLERS FOR TRMS**

4.1 FO-PID Controller	34
4.2 FOI-PD Controller	36
4.3 IO-PID Controller	38
4.4 Problem Formulation and Objective Function Optimization	39
4.5 Objective Function Optimization	40

## **CHAPTER-5**

### **RESULT AND DISCUSSION**

5.1 Real Time Results (FO-IPD)	44
5.2 Real Time Results (FO-PID)	44
5.3 Real Time Results (IO-PID)	48
5.4 Comparative analysis of FO-PID, FOI-PD & IO-PID controllers	50

<b>CHAPTER-6</b>	
6.1 CONCLUSION	51
6.2 FUTURE SCOPE	51
<b>REFERENCES</b>	52

## LIST OF FIGURES

Figure 2.1	TRMS mechanical unit	4
Figure 2.2	TRMS electro-mechanical unit	5
Figure 2.3	TRMS phenomenological unit	6
Figure 2.4	TRMS schematic MIMO model	7
Figure 2.5	TRMS non-linear Simulink model	8
Figure 3.1	Feedback control structure	19
Figure 3.2	Fractional order PID controller	25
Figure 3.3	Range of $\lambda$ and $\mu$	26
Figure 3.4	Response of step input to the plant	29
Figure 4.1	Control scheme using FO-PID for TRMS	34
Figure 4.2	Pitch angle Control using FO-PID	35
Figure 4.3	Yaw angle Control using FO-PID	35
Figure 4.4	Control scheme using FOI-PD Controller	36
Figure 4.5	Pitch angle Control using FOI-PD	37
Figure 4.6	Yaw angle Control using FOI-PD	37
Figure 4.7	Pitch angle Control using IO-PID	38
Figure 4.8	Yaw angle Control using IO-PID	38
Figure 5.1	FOPID Pitch Angle Plot (without disturbance)	44
Figure 5.1	FOPID Pitch Angle Plot (with disturbance)	44
Figure 5.1	Yaw Angle Control (without disturbance)	45
Figure 5.1	Yaw Angle Control (with disturbance)	45
Figure 5.5	FOI-PD Pitch Angle Plot (without disturbance)	46
Figure 5.6	FOI-PD Pitch Angle Plot (with disturbance)	46
Figure 5.7	FOI-PD Yaw Angle Plot (without disturbance)	47
Figure 5.8	FOI-PD Yaw Angle Plot (with disturbance)	47
Figure 5.9	IO-PID Pitch Angle Plot (without disturbance)	48
Figure 5.10	IO-PID Pitch Angle Plot (with disturbance)	48
Figure 5.11	IO-PID Yaw Angle Plot (without disturbance)	49
Figure 5.12	IO-PID Yaw Angle Plot (with disturbance)	49



## LIST OF TABLES

Table 2.1	TRMS Parameters	7
Table 4.1	Range taken for the Controller parameters-I	41
Table 4.2	Range taken for the Controller parameters-II	41
Table 4.3	Optimized IO-PID Controller parameter values-I	41
Table 4.4	Optimized IO-PID Controller parameter values-II	42
Table 5.1	Comparative analysis of FO-PID, FOI-PD & IO-PID controllers	42

## LIST OF ACRONYMS

UAV	Unmanned Aerial Vehicles
TRMS	Twin Rotor MIMO System
MIMO	Multiple- Input- Multiple Output
SISO	Single-input-single-output
PID	Proportional-integral-differential
LQR	Linear Quadratic Regulator
LQG	Linear Quadratic Gaussian
FO-PID	Fractional Order PID
FOI-PD	Fractional Order Integral-Proportional Differential
IO-PID	Integral Order PID

## ABSTRACT

A dynamical model for the characterization of a one-degree-of freedom Twin Rotor MIMO system (TRMS) in hover is depicted using a black-box system identification technique. It has striking similarity like Helicopter but it does not fly. Modelling of such complex air vehicle is very daunting task as it has a significant cross coupling between its horizontal & vertical directional motions. Therefore, it is an interesting control and identification problem. Identification for a 1-DOF rigid-body, discrete time linear model is presented in detail. In this paper, a Fractional Order Integral–Proportional Derivative (FOI-PD) controller has been realized and implemented in both simulation and real-time for the control of pitch and yaw angle of the TRMS. The novelty of the present work lies in the implementation of the robust FOI-PD controller. The nonlinear interior point optimization technique (*fmincon* function available in MATLAB optimization toolbox) has been utilized to identify the suitable controller parameter values by minimizing the cost functions within a predefined interval of controller parameters. In order to assess the performance of closed loop control system a continuously varying reference trajectory has been taken which is tracked by actual response. It is found in real time study that the FOI-PD controllers perform better than fractional order PID followed by integer order PID (IOPID) controllers based on same design criteria.

# CHAPTER-1

## INTRODUCTION

### 1.1 GENERAL

Nowadays, there has been a remarkable interest in Unmanned Aerial Vehicles (UAVs). The Twin Rotor Motor system (TRMS) also has striking similarity like a helicopter, but it does not fly. The Helicopter is a highly non-linear system having unstable system dynamics. The main and tail rotors provide horizontal and vertical movement due to which it is lifted in the air. To land and take off vertically make it unique from others, due to this capability it has generally used in various tasks such as law enforcement and border patrolling, rescue operations, firefighting, terrain surveying, cinematography, etc. The main difficulties in designing the controllers for TRMS are the cross-couplings and non-linearity's present in the system. The controllers proposed by various researchers are based on the linearized model or the other linearization technique. These linearized models are locally stable, but they are globally unstable when external disturbances are present. The Twin rotor MIMO system consists of a beam mounted on its base such that it moves freely in both lateral and longitudinal planes. It has two rotors the pitch and the yaw located at both ends of the beam which is driven by DC servo motors. A counterbalance arm weighting the end is fixed to the beam at the pivot.

The beam state is described by four process variables, the longitudinal & the lateral angles which are measured by encoders situated at the pivot and two angular velocities of the rotors, measured by speed tachometers attached to DC motors. The TRMS also has striking similarity like a helicopter, but it does not fly. The Helicopter is a highly non-linear system having unstable system dynamics. The TRMS experimental setup is used to study flight dynamics and thus can be implemented for performing experiments with air vehicles.

### 1.2 LITERATURE REVIEW

TRMS is a non-linear model, and hence, the system identification technique is used for linearization[1]. The TRMS is benchmarked system to test various controllers, and control algorithms on a real-time environment. The modeling is done with no prior knowledge of the structural model, i.e., black-box modeling. The black box modeling is based on the analysis of input and output signal of the plant. Natheer Almtireen et al. studied the PID and LQR controllers through a simulation approach for a TRMS plant[2]. Peng Wen and W.Lu explain the identification and linearization of non-linear TRMS model, which is decoupled as (SISO) single-input-single-output systems, the cross-couplings between its twin rotors are considered as disturbances to each other [3]. Rajalakshmi and Manoharan presented the

untuned PID controller for a non-linear multi-input multi-output system (MIMO) based on the linearized model[4]. Darus et al. presented System identification technique using parametric linear approaches for modeling a twin-rotor multi-input multi-output system (TRMS) is hovering position and utilizes a genetic algorithm (GA) optimization technique for dynamic modeling of a highly non-linear system[5]. Suruz Miah et al. explores the design of a generalized feedback control operator coupled with state estimation for a twin-rotor MIMO system (TRMS) intended to regulate its predefined configurations (i.e., pitch and yaw)[6]. Valluru et al. designed two loops PID controllers tuned using frequency response, Linear Quadratic Regulator (LQR), LQG controllers are designed, and also LQR and LQG are full state feedback controllers in which the performance matrices Q and R are calculated. The results are compared with the PID controller, and it is found that the optimal controller, i.e., LQG and LQR, gives better performance in terms of overshoot, settling time, and robustness[7]. Debdoot Sain et al. presents performance analysis in real-time for Fractional Order I-PD (FOI-PD) controller for TRMS. In this (FOI-PD) fractional-order Integral-Proportional Derivative controller has been designed and implemented in simulation as well as in real-time for TRMS. The optimization technique, namely (*fmincon* function available in MATLAB optimization toolbox), has been used for identifying the appropriate controller parameter by minimizing the cost function[8].

### 1.3 THESIS ORGANIZATION

Chapter one presents the detailed introduction of the benchmarked Twin rotor MIMO system along with its unstable system dynamics. The vertical and horizontal movement operation of TRMS has been explained along with non-linearities due to cross-coupling between the two rotors. This chapter additionally consists of a literature review and organization of the thesis. Chapter two consists of the descriptive model of Twin rotor MIMO system in which its mechanical as well electrical unit is explained in details along with their figures. In this chapter, mathematical modeling of TRMS model is done, and its momentum equations for the vertical and horizontal plane is derived. After that from the TRMS non-linear simulation model, the transfer function for pitch and yaw rotor are obtained and linearized. Finally, the state-space representation of the TRMS model is obtained in the form of matrix A, B, and C. Chapter three gives an overview of designing controllers for TRMS. In this, designing of FO-PID, IO-PID, and FOI-PD controller has been done along with detailed mathematical equations. Advantages and disadvantages of these controllers are also described. Finally, tuning methods of controller parameters are discussed.

Chapter four presents the experimental implementation of FO-PID, IO-PID, and FOI-PD controllers on Twin rotor MIMO system in detail. The problem is formulated, and optimized values of controller parameters are obtained and shown in tabular form.

Chapter five presents the results and discussion, which consists of the real-time response of various controllers. A comparative analysis of all the controllers is discussed in tabular form. Chapter six presents the conclusion of the work done, i.e. designing and experimental implementation of various controllers on Twin rotor MIMO system followed by future work.

## CHAPTER 2

### MODELING OF TRMS

#### 2.1 TRMS DESCRIPTION

The TRMS setup described in this section refers to the mechanical part and control unit. The mechanical and electrical connection interface shows how to measure and transfer the signals to the PC from the TRMS. In **Fig.2.1**, the TRMS mechanical part comprises two rotors which are placed on a beam together with a counterbalance. The whole set up is attached to a tower which allows safe helicopter experiments.

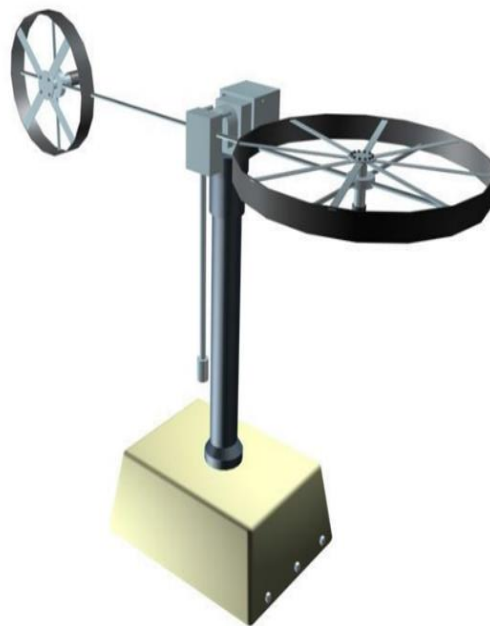


**Figure 2.1 TRMS mechanical unit**

The electrical system (positioned under the tower) performs a significant function for TRMS control apart from the mechanical systems. It enables the transfer of recorded data to the PC and the implementation of control signals via an I/O panel. A fully controlled environment is provided to TRMS by the mechanical and electrical units. The TRMS design consists of a beam mounted at its base that rotates freely in the horizontal and vertical planes. At both ends of the beam, there are two rotors, the main and the tail, driven by DC motors. A counterbalance frame is attached to the beam at the pivot with a weight at its bottom. Four process variables describe the state of the beam: horizontal and vertical angles measured by pivot-fitted encoders and their two respective angular velocities. There are also two other state variables, the linear rotor velocities, which are evaluated by velocity sensors connected with driving DC motors.

The fundamental difference between the lab set-up and the real helicopter is that the aerodynamic force is regulated by altering the angle of attack in a helicopter while the angle of attack is fixed in the lab set-up. The aerodynamic force can be controlled in the TRMS model by changing the velocity of the two rotors. Since each rotor affects both the angles position, a significant cross-coupling between these rotors can be observed.

The controller's design is based on the decoupled model to stabilize the TRMS. The TRMS scheme was designed to work with PC-based digital controller externally. Control computers are used to communicate with the position, speed sensors, and motors via a dedicated I/O board and power interface. Software operating in real-time in the MATLAB/Simulink environment responsible for controlling the I/O board.

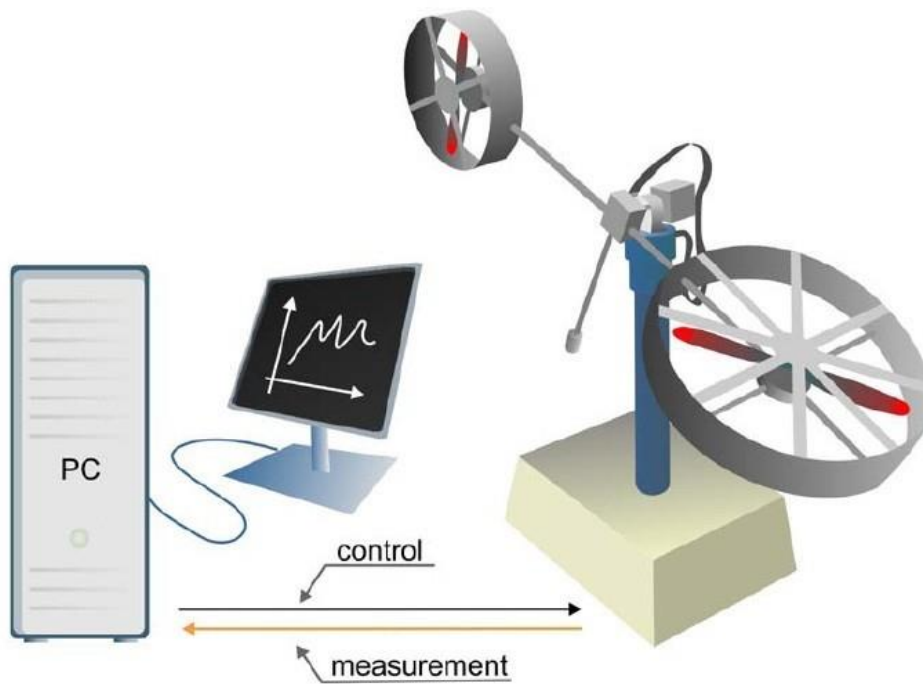


**Figure 2.2 TRMS electro-mechanical unit**



## 2.2 TRMS MATHEMATICAL MODELING

The electro-mechanical phenomenological model of the TRMS is shown in **Fig. 2.3**

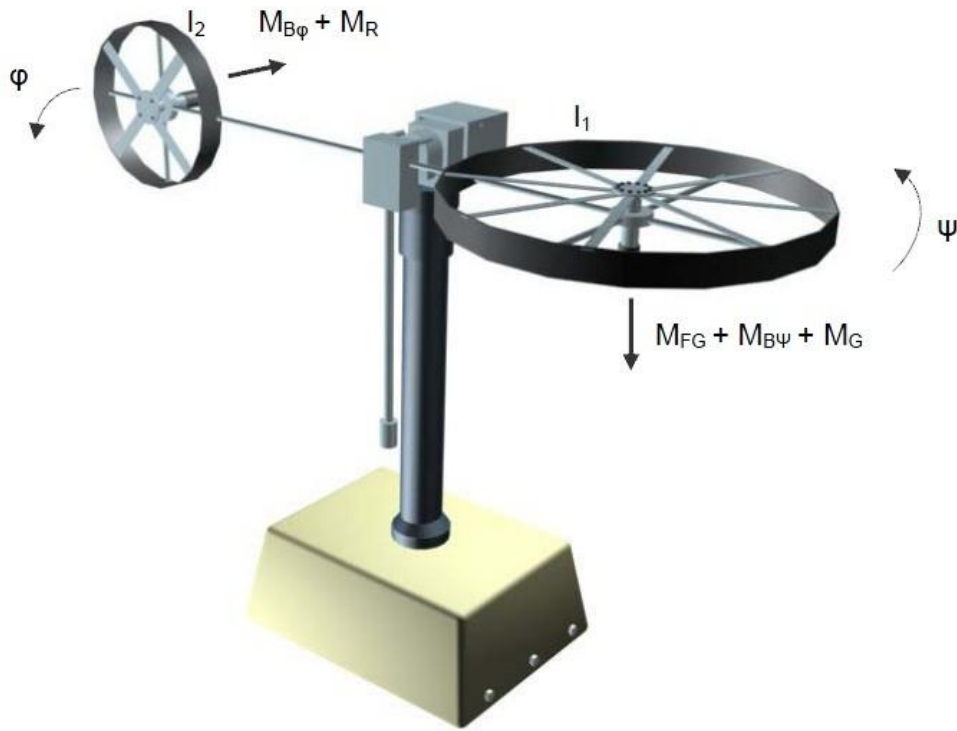


**Figure 2.3 TRMS phenomenological model**

Usually, phenomenological designs tend to be nonlinear, meaning that at least one of the states ( $i$ –rotor current,  $\theta$  –position) is a non-linear function. It must be linearized to present such a model in the form of the transfer function. The previous non-linear model equations can be obtained, as illustrated in the electrical-mechanical diagram in Figure 2.3.

For vertical movement the following momentum equation can be written as:

$$I_1 \ddot{\psi} = M_1 - M_{FG} - M_{B\psi} - M_G \quad (1)$$

Where

$$M_1 = a_1 \tau_2 + b_1 \tau_1 \quad \text{--nonlinear characteristics} \quad (2)$$

$$M_{FG} = M_g \cdot \sin \psi \quad \text{-- gravity momentum} \quad (3)$$

$$M_{B\psi} = B_{1\psi} \cdot \psi + B_{2\psi} \cdot \text{sign}(\dot{\psi}) \quad \text{-- frictional force momentum} \quad (4)$$

$$M_G = K_{gy} \cdot M_1 \cdot \dot{\phi} \cdot \cos \psi \quad \text{-- gyroscopic momentum} \quad (5)$$

A first-order transfer function approximates the motor and electrical control circuit, thus in  $s$ - domain the motor momentum is described by

$$\tau_1 = \frac{k_1}{T_{11} + T_{10}} \cdot u_1 \quad (6)$$

For horizontal plane motion, the equations are:

$$I_2 \cdot \ddot{\varphi} = M_2 - M_{B\varphi} - M_R \quad (7)$$

$$M_2 = a_2 \cdot \tau_2^2 + b_2 \cdot \tau_2 \quad (8)$$

$$M_{B\psi} = B_{1\varphi} \cdot \dot{\psi} + B_{2\varphi} \cdot \text{sign}(\dot{\varphi}) \quad (9)$$

The cross-reaction momentum  $M_R$  is approximated by

$$M_R = \frac{k_c(T_0s + 1)}{T_p s + 1} \cdot \tau_1 \quad (10)$$

Again, the DC motor with the electrical circuit is given

$$\tau_2 = \frac{k_2}{T_{21}s + T_{20}} \cdot u_2 \quad (11)$$

**Table 2.1 TRMS Parameters**

Parameters	Value
<b>I<sub>1</sub> – vertical rotor moment of inertia</b>	6.8.10 <sup>-2</sup> kg-m <sup>2</sup>
<b>I<sub>2</sub> – horizontal rotor moment of inertia</b>	2.10 <sup>-2</sup> kg-m <sup>2</sup>
<b>a<sub>1</sub> – static characteristic parameter</b>	0.0135
<b>b<sub>1</sub> – static characteristic parameter</b>	0.0924
<b>a<sub>2</sub> – static characteristic parameter</b>	0.02
<b>b<sub>2</sub> – static characteristic parameter</b>	0.09
<b>M<sub>g</sub> – gravity momentum</b>	0.32 N-m
<b>B<sub>1ψ</sub> – friction momentum function parameter</b>	6.10 <sup>-3</sup> N-m. s/rad
<b>B<sub>2ψ</sub> – friction momentum function parameter</b>	1.10 <sup>-3</sup> N-m. s <sup>2</sup> /rad
<b>B<sub>1φ</sub> – friction momentum function parameter</b>	1.10 <sup>-1</sup> N-m. s/rad
<b>B<sub>2φ</sub> – friction momentum function parameter</b>	1.10 <sup>-2</sup> N-m. s <sup>2</sup> /rad
<b>K<sub>gy</sub> – gyroscopic momentum parameter</b>	0.05 s/rad
<b>k<sub>1</sub> – motor 1 gain</b>	1.10
<b>K<sub>2</sub> – motor 2 gain</b>	0.80
<b>T<sub>11</sub> – motor 1 denominator parameter</b>	1.10
<b>T<sub>10</sub> – motor 1 denominator parameter</b>	1.0
<b>T<sub>21</sub> – motor 2 denominator parameter</b>	1.0
<b>T<sub>20</sub> – motor 2 denominator parameter</b>	1.0
<b>T<sub>p</sub> – cross reaction momentum parameter</b>	2.0
<b>T<sub>o</sub> – cross-reaction momentum parameter</b>	3.5
<b>k<sub>c</sub> – cross-reaction momentum gain</b>	-0.2

The TRMS parameters used in the above equations are chosen experimentally, which makes the Twin rotor MIMO system a nonlinear semi-phenomenological model shown in the table

below: Since the TRMS model is a MIMO plant, i.e. multiple input multiple outputs. Figure 2.4 gives a simplified schematic representation of the TRMS.

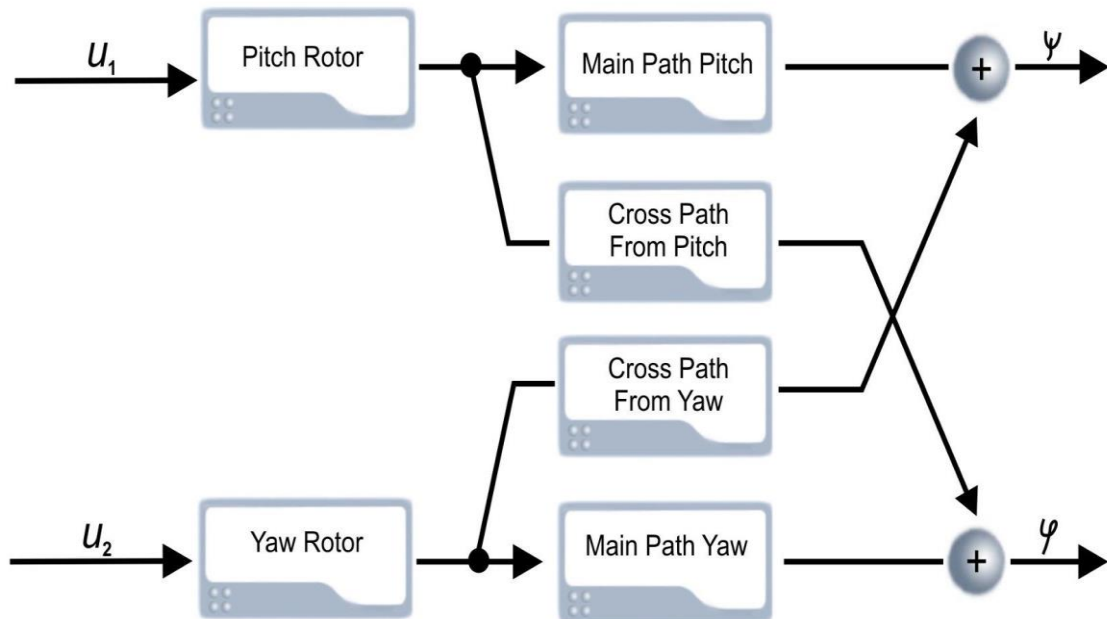


**Figure 2.4 TRMS schematic MIMO model**

Two inputs  $u_1$  and  $u_2$  control the TRMS. One of the main characteristics of the TRMS is the cross-couplings between the two rotors (Figure 2.4). The beam location is measured using incremental encoders, providing a comparative position signal. Therefore, every time the simulation of Real-Time TRMS is run, one must remember that it is important to set the proper initial conditions.

The TRMS is a nonlinear plant with important cross-couplings between the rotors, as stated in the previous chapter (Figure 2.4). The model can be treated as two linear rotor models with two linear couplings in between to keep the identification simple. Thus, four linear models are to be identified: two for the main dynamical path from  $u_1$  to  $\psi$  and  $u_2$  to  $\phi$  and others two are the cross-coupling dynamical paths from  $u_1$  to  $\phi$  and  $u_2$  to  $\psi$ . These models are used for designing the controller.

### 2.3 TWIN ROTOR MIMO SYSTEM NON-LINEAR SIMULATION MODEL

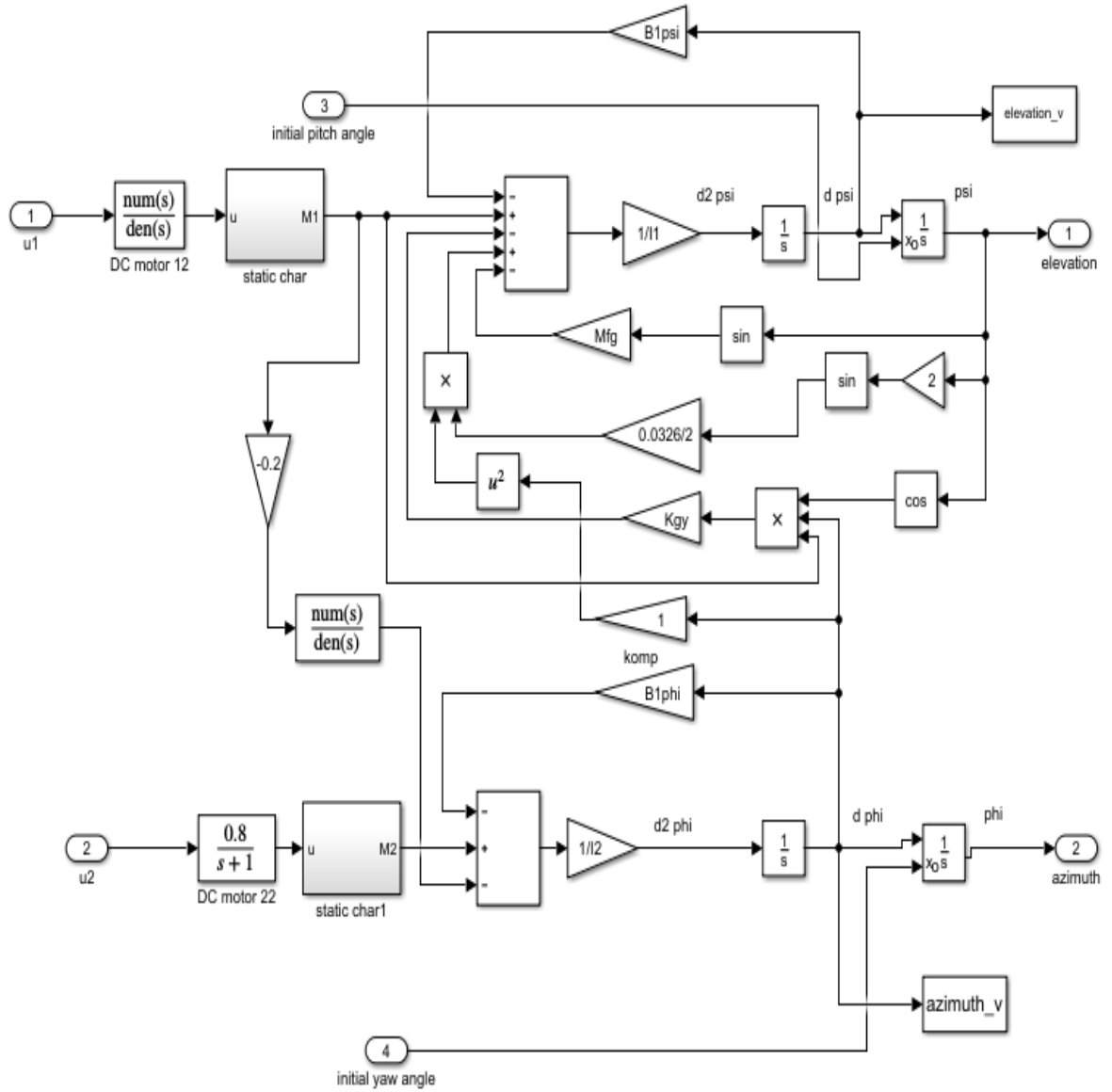


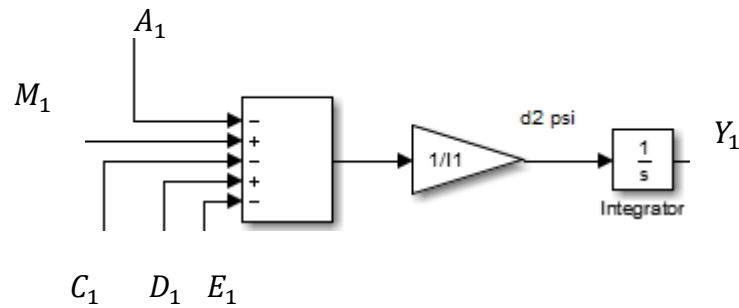
Figure 2.5 TRMS non-linear Simulink model

## 2.4 TRMS MODEL TRANSFER FUNCTION

### Step-1.

Considering our first input  $u_1$

$u_1 = \text{input } 1$



$$M_1 = b_1 \left( \frac{1.1 u_1}{1.2s + 1} \right) + a_1 \left( \frac{1.1 u_1}{1.2s + 1} \right)^2 \quad (12)$$

$$A_1 = B_1 \cdot \psi \cdot d(\psi) \quad (13)$$

$$C_1 = (k_{gy}) \cdot \cos(\psi) \cdot M_1 \cdot d(\varphi) \quad (14)$$

$$D_1 = 0.0163 \cdot \sin(2\psi) \cdot (d(\psi))^2 \quad (15)$$

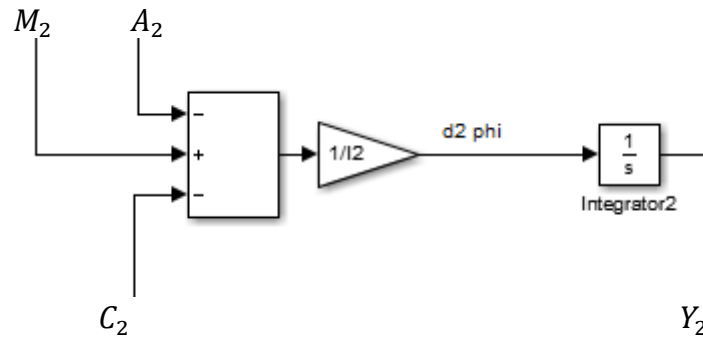
$$E_1 = M_{gf} \cdot \sin \psi \quad (16)$$

$$Y_1 = \int d(\psi) + \psi \quad (17)$$

Step-2.

Considering our second input  $u_2$

$u_2 = \text{input 2}$



$$M_2 = b_1 \left( \frac{0.8u_2}{s+1} \right) + a_2 \left( \frac{0.8u_2}{s+1} \right)^2 \quad (18)$$

$$A_2 = B_1 \phi \cdot d(\phi) \quad (19)$$

$$C_2 = -0.2M_1 \left( \frac{3.5s+1}{2s+1} \right) \quad (20)$$

$$Y_2 = \int d(\phi) + \phi_o \quad (21)$$

Step-3.

Considering our second input  $u_2$  as zero

When  $u_2 = 0$

From step 2.

$$d\phi = -\frac{1}{I_2} \left[ \int B_1 \cdot \phi \cdot d\phi + 0.2M_1 \frac{3.5s+1}{2s+1} \right] \quad (22)$$

$$d\phi = -\frac{1}{I_2} \left[ \frac{\phi^2}{2} + \int 0.2 * \frac{3.5s+1}{2s+1} * \left( b_1 \frac{1.1u_1}{1.2s+1} + a \left( \frac{1.1u_1}{1.2s+1} \right)^2 \right) \right] \quad (23)$$

Rewriting the equation (22) and (23)

$$d\varphi = -\frac{1}{I_2} \left[ \frac{\varphi^2}{2} + \int \left( \frac{0.2 * 3.5s + 1}{2s + 1} * \left( b_1 \frac{1.1u_1}{1.2s + 1} + a_1 \left( \frac{1.1u_1}{1.2s + 1} \right)^2 \right) \right) dt \right] \quad (24)$$

$$\varphi_1 = \int d\varphi + \varphi_o \quad (25)$$

From-step 1.

$$d(\psi) = \frac{1}{I_1} \left[ - \int B_1 \cdot \psi \cdot d(\psi) + \int \left( b_1 \frac{1.1u_1}{1.2s + 1} + a_1 \left( \frac{1.1u_1}{1.2s + 1} \right)^2 \right) dt \right] - \int \left( k_{gy} * \cos \psi * \left( b_1 \frac{1.1u_1}{1.2s + 1} + a_1 \left( \frac{1.1u_1}{1.2s + 1} \right)^2 \right) \cdot d\varphi \right) + \int \left( 0.0163 * \sin 2\psi \cdot (d(\varphi))^2 - \int (M_{fg} \cdot \sin \psi) dt \right) \quad (26)$$

$$d(\psi) = \frac{1}{I_1} \left[ - \int B_1 \cdot \psi \cdot d(\psi) + \int \left( 0.0163 * \sin 2\psi \cdot (d(\varphi))^2 - \int (M_{fg} \cdot \sin \psi) dt \right) \right] \quad (27)$$

$$\psi_2 = \int d(\psi) + \psi_o \quad (28)$$

From step-2.

$$d(\varphi) = \frac{1}{I_2} \left[ - \int B_1 \cdot \varphi \cdot d\varphi + \int M_2 dt \right] \quad (29)$$

$$d(\varphi) = \frac{1}{I_2} \left[ - \int B_1 \cdot \varphi \cdot d\varphi + \int \left( b_1 \frac{1.1u_1}{1.2s + 1} + a_1 \left( \frac{1.1u_1}{1.2s + 1} \right)^2 \right) dt \right] \quad (30)$$

$$\varphi_2 = \int d\varphi + \varphi_o \quad (31)$$

Step-5.

After solving the above equations and putting the system parameter values, we find SISO main pitch rotor transfer function as,

$$\text{Transfer Function} = \frac{-0.0499s^4 - 0.1703s^3 - 0.3625s^2 - 0.6952s + 0.5242}{0.0166s^4 + 0.4234s^3 + 2.6354s^2 + 2.6395s + 12.0313} \quad (32)$$

And transfer function of SISO main yaw rotor as,

$$\text{Transfer Function} = \frac{-0.0225s^4 - 0.4829s^3 - 0.6191s^2 - 0.2154s - 0.1732}{0.0010s^4 + 0.0340s^3 + 0.4205s^2 + 0.1740s + 0.0887} \quad (33)$$

But since, the TRMS is a nonlinear model that implies at least one of the states (position or rotor current) is an equation of the nonlinear function. To design the controller for controlling the TRMS, first, the mathematical model should be linearized.

## 2.5 LINEARIZED MODEL

The mathematical model presented above from equations is non-linear. To design the controller for TRMS, first, it should be linearized. The first step involves in linearization technique is finding of equilibrium points.

The following steps show the linearization technique to find equilibrium points.

The alternate model of the TRMS is given as:

$$\frac{d^2\psi}{dt^2} = \frac{(c_1\tau_1^2 + d_1\tau_1 - M_g \sin \psi) - B_1\psi \cdot \left(\frac{d\psi}{dt}\right) - B_2\psi \cdot \text{sign}\left(\frac{d\psi}{dt}\right) - k_{gy} (c_1\tau_1^2 + d_1\tau_1) \frac{d\varphi}{dt} \cos \psi}{I_1} \quad (34)$$

$$\frac{d\tau_1}{dt} = \frac{(k_1 u_1 \tau_1 T_{10})}{T_{11}} \quad (35)$$

$$\frac{d^2\varphi}{dt^2} = \frac{\left( c_2\tau_2^2 + b_2\tau_2 - B_1\varphi \cdot \left(\frac{d\varphi}{dt}\right) - B_2\varphi \cdot \text{sign}\left(\frac{d\varphi}{dt}\right) - M_R \right)}{I_2} \quad (36)$$

$$\frac{dM_R}{dt} = \frac{\left( \left( k_c - \frac{k_c T_0 T_{10}}{T_{11}} \right) \tau_1 + \frac{k_c T_0 k_1}{T_{11}} u_1 - M_R \right)}{T_P} \quad (37)$$



Now let us assume:

$$\psi = x_1 \quad (38)$$

$$\varphi = x_2 \quad (39)$$

$$\tau_1 = x_3 \quad (40)$$

$$\tau_2 = x_4 \quad (41)$$

$$M_R = x_5 \quad (42)$$

$$\frac{d\psi}{dt} = x_6 \quad (43)$$

$$\frac{d\varphi}{dt} = x_7 \quad (44)$$

Now with state-space variable, the equations in algebraic linear form can be represented as:

$$\frac{dx_1}{dt} = x_6 \quad (45)$$

$$\frac{dx_2}{dt} = x_7 \quad (46)$$

$$\frac{dx_3}{dt} = -\frac{T_{10}}{T_{11}} x_2 + \frac{k_1}{T_{11}} u_1 \quad (47)$$

$$\frac{dx_4}{dt} = -\frac{T_{20}}{T_{21}} x_4 + \frac{k_2}{T_{21}} u_2 \quad (48)$$

$$\frac{dx_5}{dt} = \frac{(k_c - \frac{k_c T_0 T_{10}}{T_{11}}) x_2}{T_p} - \frac{x_5}{T_p} + \frac{k_c T_0 k_1}{T_p T_{11}} u_1 \quad (49)$$

$$\frac{dx_6}{dt} = \frac{(c_1 x_3^2 + d_1 x_3 - M_g \sin(x_1) - B_{1x_1} x_6 - B_{2x_1} \text{sign}(x_6) - K_{gy}(c_1 x_3^2 + d_1 x_3) x_7 \cos(x_1))}{I_1} \quad (50)$$

$$\frac{dx_7}{dt} = \frac{(c_2 x_4^2 + d_2 x_4 - B_{1x_2} x_6 - B_{2x_2} \text{sign}(x_7) - x_5)}{I_2} \quad (51)$$

Now applying Taylor series for finding the equilibrium points. For this make all derivative term in equations equal to zero and then find the equilibrium point by taking  $u_1=0$  and  $u_2=0$ .

Thus, the equilibrium point will be: -

$$\begin{aligned}
x_{10} &= 0, \pi \\
x_{20} &= 0 \\
x_{30} &= 0 \\
x_{40} &= 0 \\
x_{50} &= 0 \\
x_{60} &= 0 \\
x_{70} &= 0
\end{aligned} \tag{52}$$

The non-linear equations can be represented in the state-space form given as: -

$$\dot{x} = Ax + Bu \tag{53}$$

$$y = Cx + D \tag{54}$$

Now the elements of matrix A can be obtained in the following way: -

$$\frac{dx_1}{dt} = x_6 = \frac{d\psi}{dt} \tag{55}$$

$$\frac{dx_2}{dt} = x_7 = \frac{d\varphi}{dt} \tag{56}$$

Taking  $dt = 1$ ,

On solving further, we get,

$$-\frac{M_g}{I_1} \operatorname{sign}x_6 \left( \frac{1}{x_6} \right) = \frac{dx_1}{x_1} \tag{57}$$

$$-\frac{B_2}{I_2} \operatorname{sign}x_7 \left( \frac{1}{x_7} \right) = \frac{dx_2}{x_2} \tag{58}$$

$$\frac{dx_3}{dt} = \frac{k_1 u_1 - x_3 T_{10}}{T_{11}} \tag{59}$$

$$\frac{dx_4}{dt} = \frac{k_2 u_2 - x_4 T_{20}}{T_{21}} \tag{60}$$

$$\frac{dx_5}{x_3} = \left( \frac{k_c}{T_p} - \frac{k_c T_0 T_{10}}{T_p T_{11}} \right) x_3 - \frac{x_5}{T_p} \tag{61}$$

$$\frac{dx_6}{x_6} = B_1 - B_2 \left( \frac{\operatorname{sign}x_6}{x_6} \right) \tag{62}$$

$$\frac{dx_5}{x_5} = -\frac{dt}{T_p} \quad (63)$$

$$\frac{dx_6}{x_1} = \frac{M_G \sin(x_1)}{I_1} dt \quad (64)$$

$$\frac{dx_7}{x_4} = \frac{c_2 x_4 + d_2}{I_2} \quad (65)$$

$$y = cx + d \quad (66)$$

Using these equations and putting  $u_1$  and  $u_2$  equal to 0, matrices A, B, C can be found, where matrices are defined as: -

$$A = \begin{bmatrix} \frac{dx_1}{x_1} & \frac{dx_1}{x_2} & \frac{dx_1}{x_3} & \frac{dx_1}{x_4} & \frac{dx_1}{x_5} & \frac{dx_1}{x_6} & \frac{dx_1}{x_7} \\ \frac{dx_2}{x_1} & \frac{dx_2}{x_2} & \frac{dx_2}{x_3} & \frac{dx_2}{x_4} & \frac{dx_2}{x_5} & \frac{dx_2}{x_6} & \frac{dx_2}{x_7} \\ \frac{dx_3}{x_1} & \frac{dx_3}{x_2} & \frac{dx_3}{x_3} & \frac{dx_3}{x_4} & \frac{dx_3}{x_5} & \frac{dx_3}{x_6} & \frac{dx_3}{x_7} \\ \frac{dx_4}{x_1} & \frac{dx_4}{x_2} & \frac{dx_4}{x_3} & \frac{dx_4}{x_4} & \frac{dx_4}{x_5} & \frac{dx_4}{x_6} & \frac{dx_4}{x_7} \\ \frac{dx_5}{x_1} & \frac{dx_5}{x_2} & \frac{dx_5}{x_3} & \frac{dx_5}{x_4} & \frac{dx_5}{x_5} & \frac{dx_5}{x_6} & \frac{dx_5}{x_7} \\ \frac{dx_6}{x_1} & \frac{dx_6}{x_2} & \frac{dx_6}{x_3} & \frac{dx_6}{x_4} & \frac{dx_6}{x_5} & \frac{dx_6}{x_6} & \frac{dx_6}{x_7} \\ \frac{dx_7}{x_1} & \frac{dx_7}{x_2} & \frac{dx_7}{x_3} & \frac{dx_7}{x_4} & \frac{dx_7}{x_5} & \frac{dx_7}{x_6} & \frac{dx_7}{x_7} \end{bmatrix} \quad (67)$$

$$B = \begin{bmatrix} \frac{dx_1}{u_1} & \frac{dx_1}{u_2} \\ \frac{dx_2}{u_1} & \frac{dx_2}{u_2} \\ \frac{dx_3}{u_1} & \frac{dx_3}{u_2} \\ \frac{dx_4}{u_1} & \frac{dx_4}{u_2} \\ \frac{dx_5}{u_1} & \frac{dx_5}{u_2} \\ \frac{dx_6}{u_1} & \frac{dx_6}{u_2} \\ \frac{dx_7}{u_1} & \frac{dx_7}{u_2} \end{bmatrix} \quad (68)$$

$$C = \begin{bmatrix} \frac{dy_1}{x_1} & \frac{dy_1}{x_2} & \frac{dy_1}{x_3} & \frac{dy_1}{x_4} & \frac{dy_1}{x_5} & \frac{dy_1}{x_6} & \frac{dy_1}{x_7} \\ \frac{dy_2}{x_1} & \frac{dy_2}{x_2} & \frac{dy_2}{x_3} & \frac{dy_2}{x_4} & \frac{dy_2}{x_5} & \frac{dy_2}{x_6} & \frac{dy_2}{x_7} \end{bmatrix} \quad (69)$$

Thus, on solving and putting the values, we get the matrices as:

$$A = \begin{bmatrix} -0.8333 & 0 & 0 & 0 & 0 & 0 & 0 \\ 0 & -1.0000 & 0 & 0 & 0 & 0 & 0 \\ 1.2460 & 0 & -0.0897 & -4.7060 & 0 & 0 & 0 \\ 0 & 0 & 1.0000 & 0 & 0 & 0 & 0 \\ 1.4820 & 3.6960 & 0 & 0 & -5.5000 & 0 & 18.7500 \\ 0 & 0 & 0 & 0 & 1.0000 & 0 & 0 \\ -0.0169 & 0 & 0 & 0 & 0 & 0 & -0.5000 \end{bmatrix} \quad (70)$$

$$B = \begin{bmatrix} 1 & 0 \\ 0 & 1 \\ 0 & 0 \\ 0 & 0 \\ 0 & 0 \\ 0 & 0 \\ 0 & 0 \end{bmatrix} \quad (71)$$

$$C = \begin{bmatrix} 0 & 0 & 0 & 1 & 0 & 0 & 0 \\ 0 & 0 & 0 & 0 & 0 & 1 & 0 \end{bmatrix} \quad (72)$$

$$D = \begin{bmatrix} 0 & 0 \\ 0 & 0 \end{bmatrix} \quad (73)$$

The transfer function of the linearized model of TRMS has been obtained as

$$G_p(s) = C(sI - A)^{-1}B + D = \begin{bmatrix} G_{11}(s) & G_{12}(s) \\ G_{21}(s) & G_{22}(s) \end{bmatrix} \quad (74)$$

$$\begin{bmatrix} \frac{1.2460}{(s + 0.833)(s^2 + 0.08824s + 4.706)} & 0 \\ \frac{1.4824(s + 0.2857)}{s(s + 5)(s + 0.833)(s + 0.5)} & \frac{3.60}{s(s + 5)(s + 1)} \end{bmatrix} \quad (75)$$

The above equations show clearly that the linearized model is unstable since the right half of the s-plane is the unstable region and we should note that the pole originating in the yaw transfer function shows the necessary action. The coupling effect between the two rotors input, ( $u_1$ ) pitch and the yaw angle ( $\phi$ ) also is significant.

## CHAPTER 3

### CONTROLLER DESIGN

#### 3.1 INTRODUCTION

The controller is a device that controls and changes the system parameters in the form of analog circuits or digital circuits to achieve the required performance. Basically, the controller is applicable where the system doesn't fulfill the desired results, i.e. accuracy and stability. Controllers are placed, either in parallel or series to the plant as per the requirement. A simple feedback control along with controller is shown in Figure 3.1.

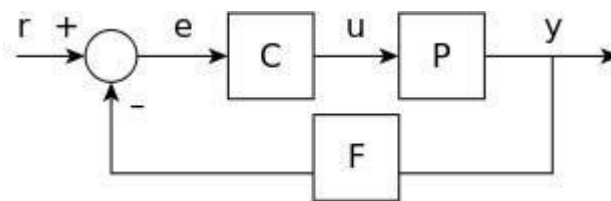


**Figure 3.1 control system feedback structure**

The error signal 'e' shows the difference between reference 'r' and the output 'y', as shown in Figure-3.1. The error signal determines the magnitude with which the output signal deviates from reference value. The controller parameter 'C' is altered and control input 'u' is applied to the plant depending on the error signal value to give satisfactory output. It needs various controllers for a plant with various inputs and various outputs. If the system is a single input and single output SISO system, the controller requires a single controller depending on the configuration of the device i.e. (physical or non-physical). By changing the input variable of the system (assuming it is MIMO) will affect the operating parameter known as the controlled output variable. It is possible to extend the concept of controllers to more complex systems. For proper operation, both natural processes and human-made systems requires controller.

### 3.2 PROPORTIONAL INTEGRAL DERIVATIVE CONTROLLER (PID)

The PID controller comprises three terms Proportional, Integral, and Derivative which represents the present errors, the accumulation of the past errors and prediction of the future errors. The PID controller comprises of 3 blocks Proportional, Integral and Derivative. The equations representing the PID controller is as follows:

$$u(t) = P.e(t) + I.\int e(t)dt + D.\frac{de(t)}{dt} \quad (76)$$

$$e(t) = y_{desired}(t) - y(t) \quad (77)$$

By taking the Laplace transform of the above equation, it can be represented as:

$$U(s) = \left( P + \frac{I}{s} + D.s \right).E(s) \quad (78)$$

$$C(s) = \frac{U(s)}{E(s)} = \left( P + \frac{I}{s} + D.s \right) = \frac{Ds^2 + Ps + I}{s} \quad (79)$$

Each of the blocks of PID controller (P, I and D) has a key role, but to obtain satisfactory results, integral or derivative part must be excluded for some applications. Mostly the Proportional block is responsible for the system reaction speed. In some plants, if the P value is set to be large, oscillations may occur. The Integral part is very essential and ensures 0 error value in steady state, indicating the output will be exactly what we want it to be. Nevertheless, the controller's integral action leads the system to respond more slowly to desired changes in values and structure.

#### 3.2.1 INTEGER ORDER PROPORTIONAL INTEGRAL DERIVATIVE (IO- PID) CONTROLLER

The integral order PID controller comprises three terms Proportional, Integral, and Derivative which represents the present errors, the accumulation of the past errors and prediction of the future errors. The PID controller comprises of 3 blocks Proportional, Integral and Derivative. The equations representing the PID controller is as follows:

$$u(t) = P.e(t) + I.\int e(t)dt + D.\frac{de(t)}{dt} \quad (80)$$

$$e(t) = y_{desired}(t) - y(t) \quad (81)$$

By taking Laplace transform of the above, it can be represented as:

$$U(s) = \left( P + \frac{I}{s} + D \cdot s \right) \cdot E(s) \quad (82)$$

$$C(s) = \frac{U(s)}{E(s)} = \left( P + \frac{I}{s} + D \cdot s \right) = \frac{Ds^2 + Ps + I}{s} \quad (83)$$

Each of the blocks of PID controller (P, I and D) has a key role, but to obtain satisfactory results, integral or derivative part must be excluded for some applications. Mostly the Proportional block is responsible for the system reaction speed. In some plants, if the P value is set to be large, oscillations may occur. The Integral part is very essential and ensures 0 error value in steady state, indicating the output will be exactly what we want it to be. Nevertheless, the controller's integral action leads the system to respond more slowly to the desired change in value and structure.

Since some non-linearities are causing problems for integral action. Therefore, to make the response faster, the derivative part has been introduced. But it is very sensitive to an increase in noise amplitude and can cause the system to react nervously. So It is often ignored in the design of the controller. Derivative part can decrease the nervous reaction, but it also slows down the controller's response. Proper filtration can help to decrease high frequency noise without decreasing the efficiency of the control system in the lower frequency band.

### 3.3 FRACTIONAL ORDER CONTROLLER (FOC)

#### 3.3.1 INTRODUCTION

Fractional order control scheme is an application of fractional calculus in control engineering. As the name suggests, unlike the integer order which moves between integer numbers (order belongs to integer numbers), the fractional order moves along the real axis whose order belongs to the real number. But it is suggested that order is between '0' and '2' for process control application. In some literatures it is mentioned that order greater than '2' in control application leads to unstable operation of system. In fractional order control there are various types of controllers such as FOPID controller, FOI-PD controller, FO-PD/PI controller, fractional lead-lag compensator, CRONE controller. FOPID controllers have acknowledged a considerable attention in the recent years. They provide more flexibility in the controller design as they have five parameters. In recent past, FOPID controllers have been proposed by 'I. Podlubny' in time domain and by 'Patras' in frequency domain which is capable of enhancing the closed loop performance of a system over an integer order controller. A FOPID controller's true prospect depends



heavily on its tuning methodology, and performance can severely degrade, with contradictory design specifications being met by fractional order controllers.

### 3.3.2 FRACTIONAL CALCULUS

Fractional calculus deals with integers and derivatives theory of numbers. It also simplifies the integer order notation and the integration of "n" folds. The derivatives and integrals of fractional order provide a powerful tool for memory description. Fractional calculus is also three centuries old like integer calculus, but is not common in the field of research. Many researchers have been using this as a tool for their research work in various fields of science and engineering such as control engineering, mechanical, chemical, signal processing etc. since the last few centuries.

### 3.3.3 DEFINITIONS OF FRACTIONAL CALCULUS

Since many definitions of fractional calculus starting with n-fold definitions to other different variations has been given.

The following fractional calculus operator is used and  ${}_{\alpha}D_t^{\alpha}$  is defined as follows:

$${}_{\alpha}D_t^{\alpha} = \begin{cases} \frac{d^{\alpha}}{dt^{\alpha}} R(\alpha) > 0 \\ 1R(\alpha) = 0 \\ \int_a^t dz^{-\alpha} R(\alpha) < 0 \end{cases} \quad \text{where } R(\alpha) \text{ refers to the real part of } \alpha. \quad (84)$$

The following definitions of fractional calculus are widely used in the various areas of control system given as follows:

#### 3.3.3.1 Grunwald-Letnikov (GL) definition:

The Grunwald-Letnikov definition is represented as:

$${}_{\alpha}D_t^{\alpha} f(t) = \lim_{h \rightarrow 0} \frac{1}{h^{\alpha}} \sum_{j=0}^{\left[ \frac{t-\alpha}{h} \right]} (-1)^j \binom{n}{j} f(t-jh) \quad (85)$$

Where 't' & 'a' are the operator limits. 'n' is the integer value satisfying the condition  $-1 < n$ .

Binomial coefficient value is given by:

$$\binom{n}{j} = \frac{\Gamma(n+1)}{\Gamma(j+1)\Gamma(n-j+1)} \quad (86)$$

And the function used in above equation i.e. gamma function is defined as:

$$\Gamma(x) = \int_0^{\infty} t^{x-1} e^{-t} dt \quad (87)$$

This definition of GL is generally used in numerical evaluations, which is very useful for finding a numerical solution of differential fractional equations.

### 3.3.3.2 Riemann-Liouville (RL) definition:

Liouville defined the arbitrary order derivative as an infinite series. The drawback is that its order must be restricted to the values for which the series converging. To obtain a formula relating the integration of an arbitrary number, Riemann used the generalization of Taylor series. It can be illustrated that the approaches suggested by Liouville can be reduced in one single formula.

It is defined as:

$${}_{\alpha} D_t^{\alpha} f(t) = \frac{1}{\Gamma(n-\alpha)} \left( \frac{d}{dt} \right)^n \int_a^t \frac{f(t)}{(t-T)^{\alpha-n+1}} dt \quad (88)$$

Where, n is an integer which satisfies the condition  $n-1 < \alpha < n$ . 'a' and 't' are the limits of integration.

The fractional integral and derivatives concept of RL is helpful for obtaining the analytical solution of simple functions such as  $e^t, t^b, \cos(t)$ .

### 3.3.3.3 M. Caputo definition

The definition given by Caputo is widely used in engineering applications because it is a direct link between the initial conditions type and the fractional derivative type.

It is stated as:

$${}_{\alpha} D_t^{\alpha} f(t) = \frac{1}{\Gamma(n-\alpha)} \int_a^t \frac{f^n(T)}{(t-T)^{\alpha-n+1}} dt \quad (89)$$

Where, n is an integer which satisfies the condition  $n-1 < \alpha < n$ . 'a' and 't' are the limits of integration.

The Laplace transform of above fractional operator is defined as:

$$L\left({}_\alpha D_t^\alpha f(t)\right) = s^\alpha F(s) \quad (90)$$

### 3.3.4 FRACTIONAL ORDER PID CONTROLLER

For many decades, the PID controller has been the most widely used process control technique. PID controllers are certainly still commonly used in industrial processes despite significant developments in control theory and technology in recent years. This is because for a wide class of processes, they show good performance. They also provide robust efficiency for a wide range of working conditions. Many possible methods were described in the literature in time and frequency domain to define the tuning parameter on suitable PID controllers. There are four possible system and controller combinations in control system theory.

- The system and controller both are integer order type.
- Fractional order system which are controlled by integer order controller.
- Fractional order system which are controlled by fractional order controller.
- Integer order system which are controlled by fractional order controller.

Since the majority of the systems are modelled as integer order ones, fourth one type of combination is most popular.

FOPID (fractional form PID) is a stage further in PID controllers. Over the past two decades, FOPID controllers have gained considerable attention. Compared to conventional PID controllers, they provide more flexible in controller design. This is because there are five parameters in FOPID than standard PID controllers where only three parameters are selected. This flexibility also suggests that the controller's tuning may be much more complex. FOPID controller is proposed by I. Podlubny in 1994. They are able to improve a system's closed loop performance over a simple Integer order PID structure. This is because in the case of conventional PID controllers they have three parameters to select where as there are five in FOPID. FOPID controller design is simple and performance shown by them are good. For slow process systems, they will give less overshoot percentage and less settling time. A Fractional order device can easily attain Iso-damping properties. The system is said to have iso-damping properties if it provides a flat line at a frequency called "Tangent frequency" in the phase plot in Bode plot. It implies that the derivative of phase function w.r.t frequency results to zero at the frequency called tangent frequency. Systems with this property have constant over-shoot in closed loop step response for different values of control gain i.e.

Systems are robust against variations in gain. Fractional PIDs are from PIDs generation and its output is a linear combination of input, a fractional integral of the input, and a fractional derivative of input.

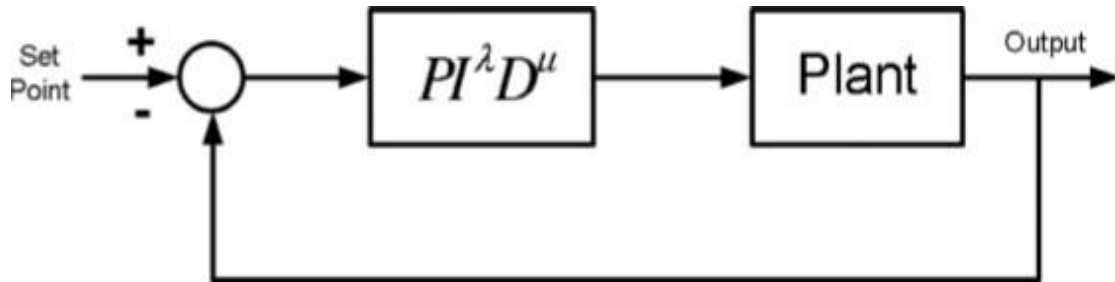


**Figure 3.2 fractional order PID controller**

The equation of generalized transfer function of fractional PID controller is given by:

$$C(s) = \frac{U(s)}{E(s)} = \left( k_p + \frac{k_i}{s^\lambda} + k_d s^\mu \right) \quad (91)$$

Where,  $(\lambda, \mu \geq 0)$

Where the controller output is  $C(s)$ , the control signal is  $U(s)$ , the error signal is  $E(s)$ , the proportional constant gain is  $K_p$ , the integral constant gain is  $K_i$ , the derivative constant gain is  $K_d$ .  $\lambda$  is the order of integration and the order of differentiation is  $\mu$ . All conventional PID controllers of the integer order are the specific case of the PID controller of the fractional order where  $\lambda=1$  and  $\mu=1$ .

As shown in the figure below, we have to move between four points in conventional PID controllers for four different kinds of controllers (P, PI, PD, and PID). Unlike the Integer order controller, it is possible to move continuously in the plane for fractional order controllers. The range of fractional order generally varies from 0 to 2.

- If value of  $\lambda=1$  &  $\mu=1$ , then it is a classical PID controller.
- If value of  $\lambda=0$  &  $\mu=1$ , then it is a classical PD controller.
- If value of  $\lambda=1$  &  $\mu=0$ , then it is a classical PI controller.
- If value of  $\lambda=0$  &  $\mu=0$ , then it is a classical P controller.

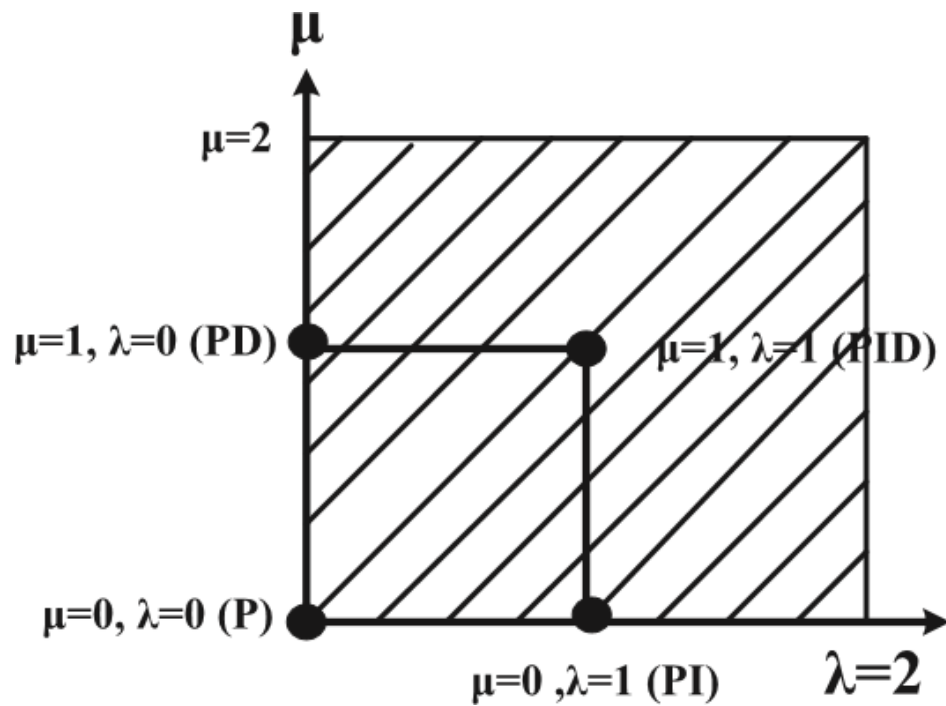


Figure 3.3 Range of  $\lambda$  and  $\mu$

### 3.3.5 ADVANTAGES OF FRACTIONAL ORDER CONTROLLER OVER AN INTEGER ORDER

- In FOPID it is possible to achieve five distinct specifications by varying five parameters, which is not possible in the case of IOPID.
- Iso-damping properties can be easily obtained by FOPID compared to IOPID.
- For higher order systems, the efficiency of the controller weakens when standard PID controllers are used. While in the case of FOPID, even with the higher order systems, it provides improved results.
- For a system with more time delay, the Fractional PID controller gives better results than conventional PID controllers.
- As fractional PID have five parameters for tuning, it is more robust and stable whereas integer order PID provides less robustness and stability.
- It is complicated and difficult to control a system that has nonlinearities using conventional PID controllers, in those cases, fractional PID controllers seem to give better.
- For the Non-minimum phase system, the fractional PID controller gives better response.
- If we work on a non-linear system, it is common practice to linearize the system at distinct operating points and then to design the controllers for distinct operating

points. But for non-linear systems, only fractional PID controller is typically sufficient.

By considering above benefits of fractional controller over conventional type, FOPID controller has following applications/situations for efficient performance:

- For Higher order systems.
- Systems which are having long time delays.
- Systems with non-linearities.
- For Non-minimum phase system.
- Systems in which we require robust stability.

### **3.3.6 DISADVANTAGE OF FRACTIONAL ORDER CONTROLLER:**

- Since there are no generalized tuning methods for the tuning of FOPID whereas for conventional PID there are various tuning techniques.
- For Obtaining the optimized five parameters of FPID by tuning is a very daunting task.

### **3.3.7 TUNING OF PID**

Tuning is the method for obtaining optimum controller parameter according to system requirements. For example, tuning will be done for getting the optimum values of  $K_p$ ,  $K_d$ , and  $K_i$  in the case of a PID controller. Whereas in case of FOPID  $K_p$ ,  $K_d$ ,  $K_i$ ,  $\lambda$  and  $\mu$ . The presence of a number of tuning techniques and the automatic tuning function that simplifies their design is one of the factors for the tremendous success of conventional PID controllers. For this purpose, many FOPID tuning methods are now being proposed by researchers in various literatures to improve the use of fractional controllers in different applications. Many researchers have proposed several tuning strategies for tuning of FO-PID controllers in both frequency and time domain specification. It was discovered that the method of frequency domain design needs a reduced order model of the original higher order process. On the other hand, reduced order model is not necessarily required for time domain tuning techniques. Therefore, higher order process model is sufficient to determine the parameters of controller through the optimization technique having time domain performance indices as the design criteria. Now a days most of industrial PID controllers are tuned to a few sets of design specifications either in time domain (error index, rise time, over-shoot percentage,

settling time, under-shoot ratio, etc.) or in frequency domain (gain margin, phase margin, cross-over frequencies, maximum sensitivity and complex sensitivity magnitudes, etc). That is why a single tuning method cannot meet all of the above design specifications, i.e. satisfying the performance specifications of the time and frequency domain at the same time. Indeed, because of over-specification, such design criteria can often give unsatisfactory and sometimes even in closed loop response. Therefore, as mentioned above, a FOPID controller that satisfies few sets of time domain specifications may not have sufficient robustness against system parameter uncertainties in frequency domain analysis and vice versa. It is evident from this discussion that each tuning strategy has its own strength and weakness inherent in it.

### **3.3.8 TUNING METHOD FOR FRACTIONAL ORDER CONTROLLER:**

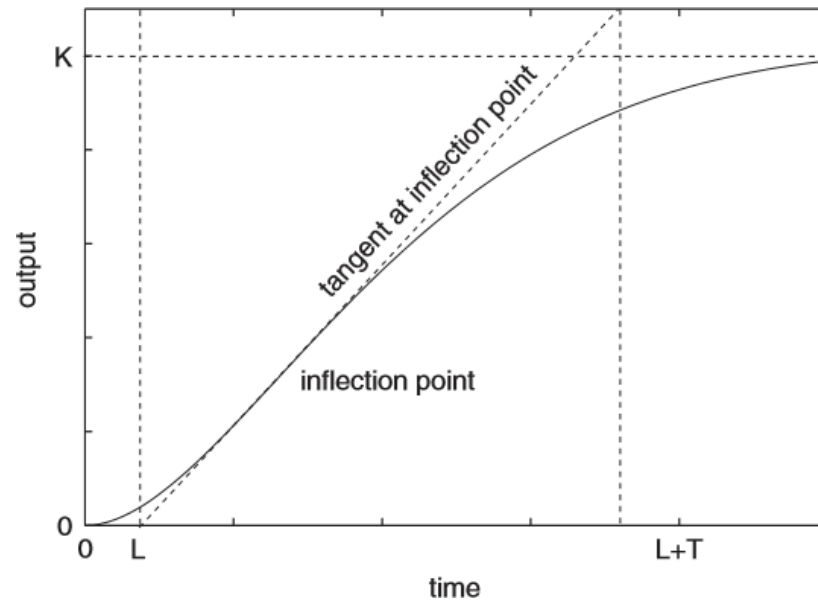
Controller tuning is always a challenging task. There are five parameters to be tuned in the case of a fractional PID controller. So, it's quite complex and difficult. According to the tuning methods proposed by D. Valerio and J. Costa, which is divided into following three different categories:

- Rule base tuning methods
- Analytic tuning methods
- Numerical tuning methods

Apart from this above-mentioned methods, two other methods self-tuning and auto-tuning can be used for tuning of fractional order controllers.

#### **3.3.8.1 Rule base methods:**

It is one of revolutionary tuning techniques for PID controllers. e.g. Ziegler-Nichols technique. The performance of the control system is enhanced in most cases, but this technique is primarily applicable for selection of the starting tuning point. The process needs step response in S-shaped curve.

**Figure 3.4 response for step input to the plant**

The figure shown above is the response for the step input to the plant (plant is of the 1<sup>st</sup>-order with some delay system). In the above figure  $L$  represents apparent delay and  $T$  is the time constant resulting from the pole. As discussed earlier that Zeigler-Nichols method can be used for tuning the controller or choosing the starting points for further tuning of the fractional order controller.

### 3.3.8.2 Analytical methods:

The controller's parameters were obtained in the analytical tuning method by solving equations. We have to find five parameters in the fractional controller so that it needs five equations created by each specification. Thus, by using those values obtained by solving equations, we can fulfill five different specifications.

### 3.3.8.3 Self tuning and Auto tuning:

A self-tuning controller contains a traditional controller as well as a self-tuning function that tries to keep optimum closed loop performance by continually updating the controller parameter. An auto tuning is equivalent except that it only executes its tuning procedure once, then initiates closed loop control using the calculated parameters. The main components of the auto-tuning algorithm are the following:

- To generate the identification input with a little or none a priori system information
- Parameter identification of the transfer function through optimization
- Verification of model
- Synthesis of Controllers
- Evaluation of performance parameters



### 3.3.9 CLASSICAL TUNING PROCEDURE FOR FRACTIONAL ORDER PI/PD CONTROLLERS:

The transfer function of fractional order PI /PD controller is defined as follow:

$$H_{FO-PI}(S) = k_p \left( 1 + \frac{k_i}{s^\lambda} \right) \quad (93)$$

$$H_{FO-PD}(S) = k_p (1 + k_d s^\mu) \quad (94)$$

Where fractional orders represented by  $\mu, \lambda \in (0, 2)$ , Proportional gain constant  $K_p$ , integral gain constant  $K_i$  and the derivative gain constant  $K_d$ . One of the most commonly used fractional order controller tuning procedures begins with a set of specifications for the frequency domain. We have to get three parameters when tuning FO PI / PD. Thus, consider three specifications for the frequency domain. The three specifications to be met by controller are as follows

#### 1. A gain crossover frequency ( $\omega_{gc}$ )

The gain crossover frequency is associated with the closed loop system's settling time. It is thus used as the controller's important tuning parameter. A large gain crossover frequency will lead in a smaller closed loop settling time. To ensure the imposed gain crossover frequency for a system, the following condition must hold

$$|H_{open-loop}(j\omega_{gc})| = 1 \quad (95)$$

Where  $H_{open-loop}(s)$  is the open loop transfer function defined as:

$$H_{open-loop}(s) = P(s) * H_{FOC}(s) \quad (96)$$

Where  $P(s)$  represents the transfer function of the process to be controlled and  $H_{FOC}(s)$  is either the FO-PI or FO-PD controller defined in (88) and (89) respectively.

#### 2. A phase margin ( $\phi_m$ )

Phase margin is a significant measure of the stability of a system and an indicator of the overshoot of the closed loop. An interval between  $45^\circ$  and  $65^\circ$  is usually used to select a proper phase margin. In order for a system to ensure a certain phase margin, the following condition must satisfy:

$$\angle H_{open-loop}(j\omega_{gc}) = -\pi + \phi_m \quad (97)$$

### 3. Iso-damping property:

This condition guarantees that the system is more robust in order to gain changes and that the overshoot of the response within a gain range is almost constant. A steady phase margin across the desired gain crossover frequency must be maintained to ensure a constant overshoot, which eventually means that the open loop system phase must be kept constant around the specified. In order for a system to ensure the Iso-damping property, the following condition must be satisfied

$$\left. \frac{d(\angle H_{open-loop}(j\omega_{gc}))}{d\omega} \right\}_{\omega=\omega_{gc}} = 0 \quad (98)$$

The complex representation in the frequency domain of the transfer functions describing the FO-PI or FO-PD are as follows:

$$H_{FO-PI}(j\omega) = k_p \left[ 1 + k_i \omega^{-\lambda} \left( \cos \frac{\pi\lambda}{2} - j \sin \frac{\pi\lambda}{2} \right) \right] \quad (99)$$

$$H_{FO-PD}(j\omega) = k_p \left[ 1 + k_d \omega^{\mu} \left( \cos \frac{\pi\mu}{2} - j \sin \frac{\pi\mu}{2} \right) \right] \quad (100)$$

The corresponding magnitudes of above two equations are as follows:

$$|H_{FO-PI}(j\omega)| = k_p \sqrt{2k_i \omega^{-\lambda} \cos \frac{\pi\lambda}{2} + k_i^2 \omega^{-2\lambda}} \quad (101)$$

$$|H_{FO-PD}(j\omega)| = k_p \sqrt{2k_d \omega^{\mu} \cos \frac{\pi\mu}{2} + k_d^2 \omega^{-2\mu}} \quad (102)$$

The phase of the equations and is as follows:

$$\angle H_{FO-PI}(j\omega) = -a \tan \left( \frac{k_i \omega^{-\lambda} \sin \frac{\pi\lambda}{2}}{1 + k_i \omega^{-\lambda} \cos \frac{\pi\lambda}{2}} \right) \quad (103)$$

$$\angle H_{FO-PD}(j\omega) = a \tan \left( \frac{k_d \omega^{\mu} \sin \frac{\pi\mu}{2}}{1 + k_d \omega^{\mu} \cos \frac{\pi\mu}{2}} \right) \quad (104)$$

Now consider FO-PI controller and by applying three frequency domain specifications on it the equations got are as follows:

- When we apply gain crossover frequency condition on FO-PI controller

$$k_p \sqrt{1 + 2k_i \omega_{gc}^{-\mu} \cos \frac{\pi\lambda}{2} + k_i^2 \omega_{gc}^{-2\lambda}} = \frac{1}{|P(\omega_{gc})|} \quad (105)$$

- When we put a phase margin constraint

$$\frac{k_i \omega_{gc}^{-\lambda} \sin \frac{\pi\lambda}{2}}{1 + k_i \omega_{gc}^{-\lambda} \cos \frac{\pi\lambda}{2}} = \tan(\pi - \phi_m + \angle P(j\omega_{gc})) \quad (106)$$

- When we apply Iso damping property on FO-PI controller

$$\left. \frac{\lambda k_i \omega_{gc}^{-\lambda-1} \sin \frac{\pi\lambda}{2}}{1 + 2k_i \omega_{gc}^{-\lambda} \cos \frac{\pi\lambda}{2} + k_i^2 \omega_{gc}^{-2\lambda}} + \frac{d\angle P(j\omega)}{d\omega} \right\}_{\omega=\omega_{gc}} = 0 \quad (107)$$

For proper tuning of the FO-PI controller, the system of nonlinear equations (100)-(102) to be solved by using either graphical methods or optimization techniques.

### 3.3.10 OPTIMIZATION TECHNIQUE:

The MATLAB has a optimization toolbox which can be used for optimization techniques, the feature '*fmincon*' for which the condition of the modulus in (105) can be used as the function to minimize i.e. objective function. While the condition of the phase in (106) and the condition of robustness (Iso damping property) in (107) are the non-linear constraints.

It is also necessary to specify initial values of the controller parameters, having the possibility of setting the lower and upper boundaries as well. The '*fmincon*' function returns the controller parameters (in this case the controller parameters are  $K_p$ ,  $K_i$  and  $\lambda$ ) so that the modulus condition (105)-(107) is minimized and the nonlinear constraints are met.

### 3.3.11 GRAPHICAL METHOD:

This technique involves evaluating the parameter of  $K_i$  as a function of the fractional order  $\mu$ . Then the corresponding  $K_i$  values are calculated for different values of  $\mu$  (varies from 0 to 2). The graphical method then comprises of plotting different values of  $K_i$  which are derived

from the equation. Similarly, another graph for different values of  $K_i$  is computed on the same plot for the different values of  $\mu$ . Then we get a point of intersection between the two plots. The final values of  $K_i$  and  $\mu$  parameters are that intersection point. Now compute the final value of  $K_p$  using the initial values of  $K_i$  and  $\mu$  by satisfying the modulus condition (105).

## CHAPTER 4

### CONTROL SCHEME USING FO-PID, FO-I-PD & IO-PID CONTROLLERS FOR TWIN ROTOR MIMO SYSTEM

#### 4.1 FO-PID CONTROLLERS:

The FOPID controller originated from the fractional calculus that is as old as its counterpart i.e. integer order. It was difficult to deal with due to very complex mathematical expressions of fractional order differential-integral operators. But in recent years, some techniques have been proposed describing how to use fractional calculus to solve differentiation and integration problems. In 1999, Podlubny introduced first significant work on FOPID controllers. Some of the commonly used phrases are described in Chapter 3 by Riemann-Liouville, Grunwald-Letnikov and Caputo. The control scheme using FO-PID controller is shown in figure 2 below:

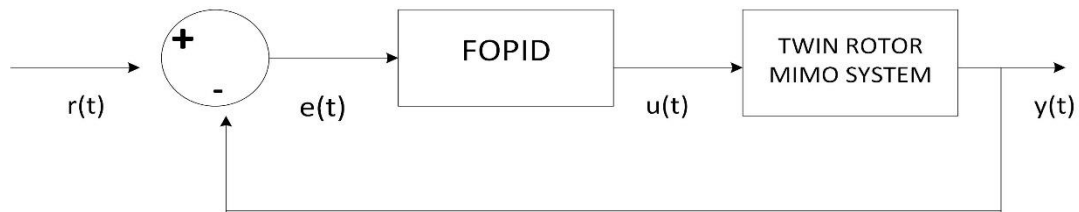


**Figure 4.1 control scheme using FO-PID for TRMS**

The FO-PID controller is in the form of

$$u(t) = k_p e(t) + k_i D^{-\lambda} e(t) + k_d D^{\mu} e(t) \quad (108)$$

Where  $k_p$ ,  $k_i$ , and  $k_d$  represents proportional, integral and derivative terms same as in IO-PID controller but FO-PID controller has two extra terms  $\lambda$  and  $\mu$  from fractional differentiation and integration associated with the second and third term of (103). The FOPID expression in s-domain can be obtained through (104) as:

$$C(s) = \frac{U(s)}{E(s)} = \left( k_p + \frac{k_i}{s^{\lambda}} + k_d s^{\mu} \right) \quad (109)$$

The  $\lambda$  and  $\mu$  values vary from 0 to 1. The FOPID acts as an IO-PID device for  $\lambda = 1$ ,  $\mu = 1$ . It can therefore be concluded that FOPID is more flexible than the IOPID controller. The FOPID differential and integral terms are approximated to integer values using the approximation of Oustaloup's 5th order for optimal tuning and desired results.

**Figure 4.2 Pitch angle control using FO-PID**

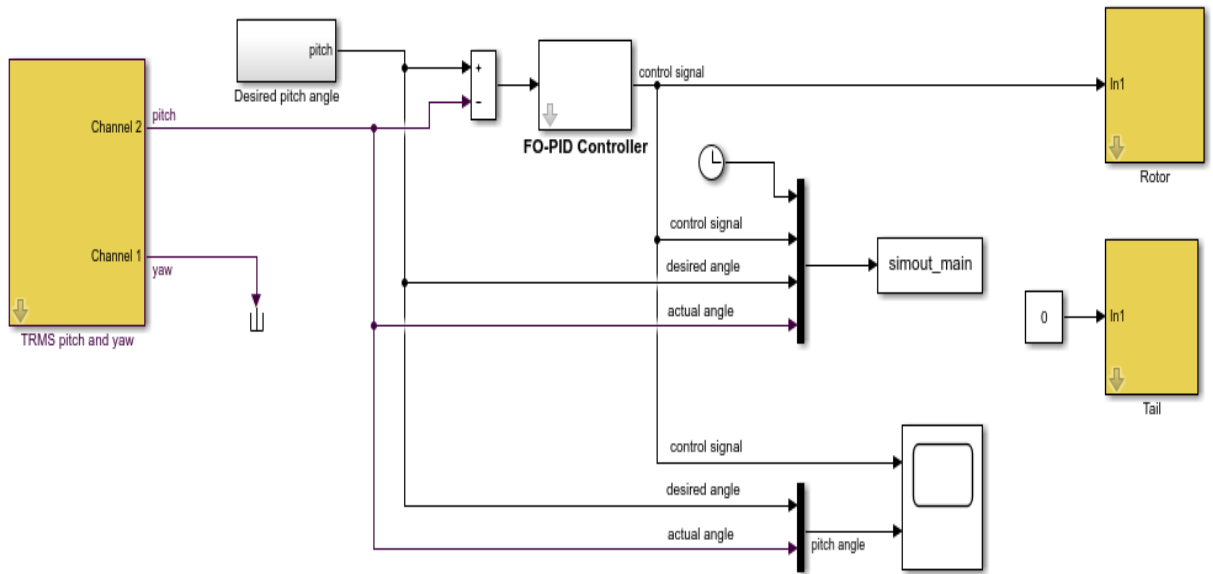
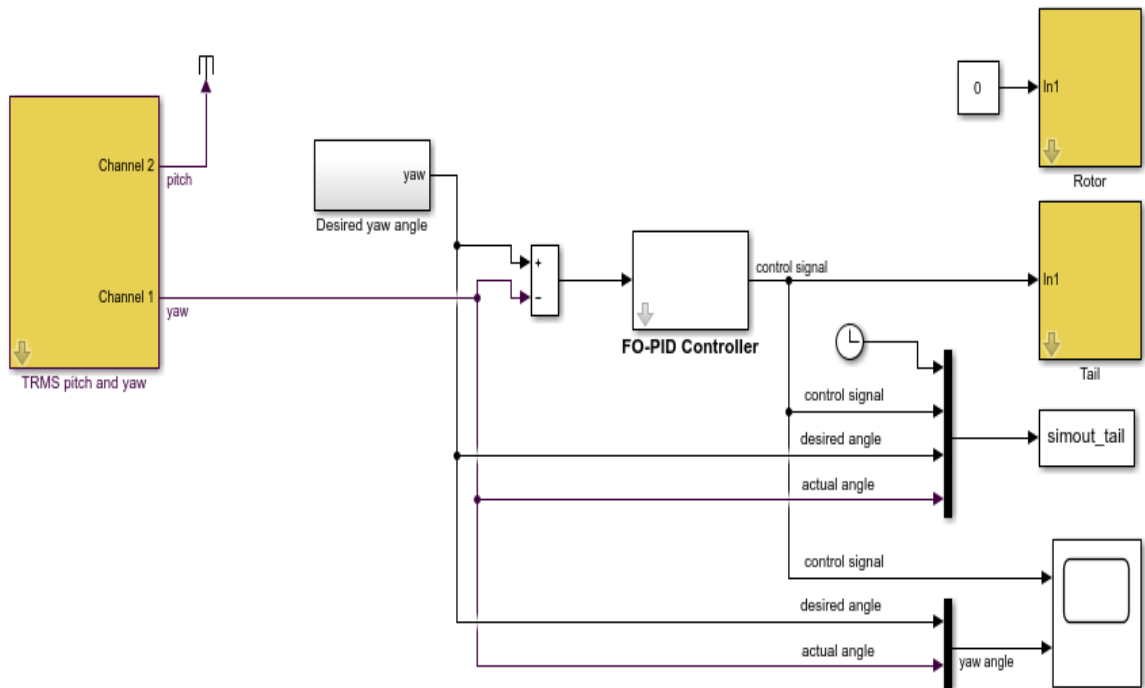


**Figure 4.3 Yaw angle control using FO-PID**



## 4.2 FOI-PD CONTROLLERS

It is simple modification in the existing conventional PID controller. The (P-D) proportional and derivative blocks are kept up in the path of feedback whereas the integral (I) block is placed in the forward path. The I-PD controller's higher flexibility in satisfying the design criteria accurately is due to the presence of various signal paths for the process output and the set-point. In Figure the structure of the FOI-PD controller is provided.

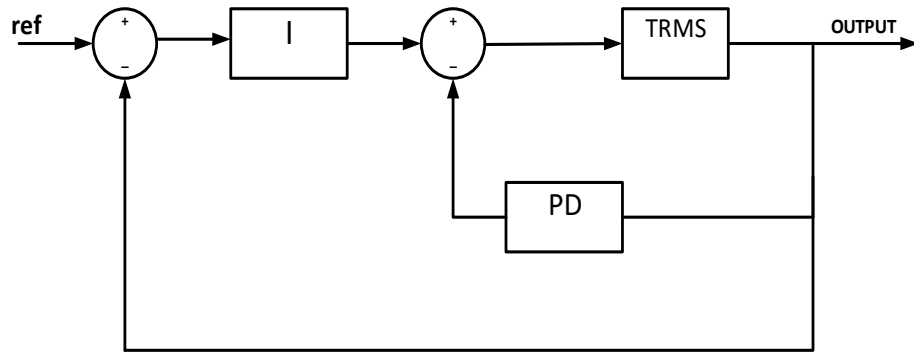


**Figure 4.4 control scheme for FOI-PD controller**

The characteristic equation of the TRMS plant with IOI-PD controller for unity feedback is given by:

$$1 + G_p(s)(G_{C1}(s) + G_{CPD}(s)) = 0 \quad (110)$$

*i.e.*

$$1 + G_p(s) \left( \left( \frac{k_i}{s} \right) + (k_p + k_d s) \right) = 0 \quad (111)$$

Characteristic equation of the system with FOI-PD controller for unity feedback is given by:

$$1 + G_p(s) \left( \left( \frac{k_i}{s^\lambda} \right) + (k_p + k_d s^\beta) \right) = 0 \quad (112)$$

Where  $\lambda$  and  $\mu$  are the fraction power of  $s$ .

**Figure 4.5 Pitch angle control using FOI-PD**

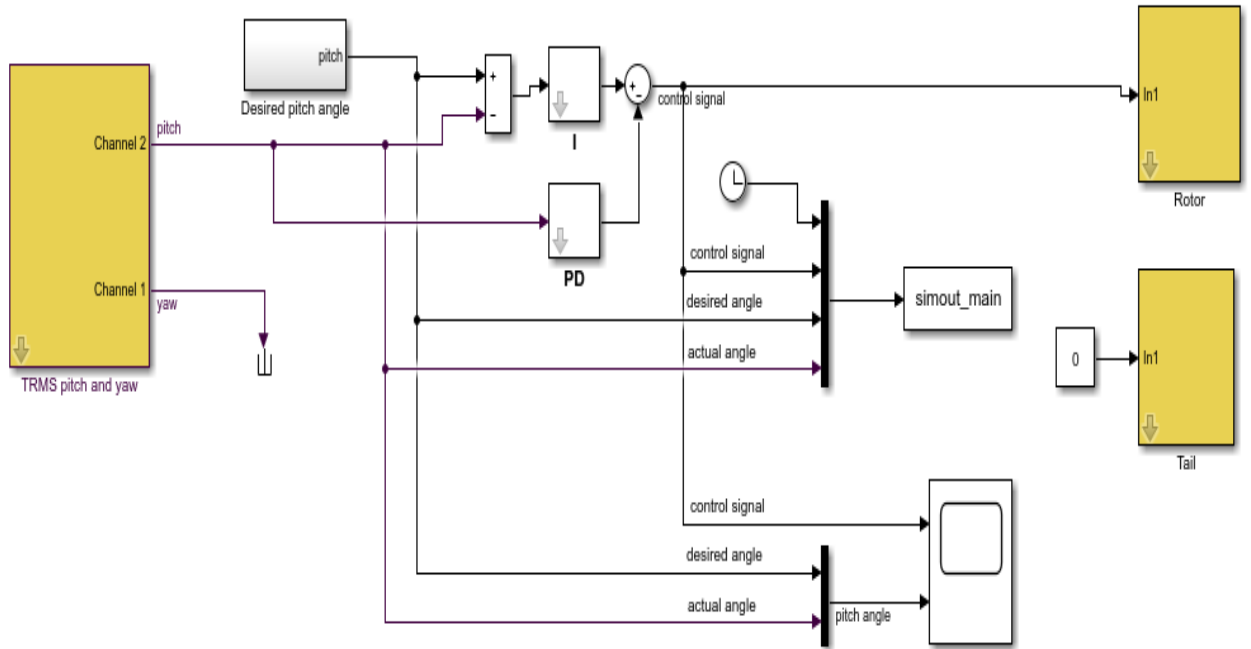
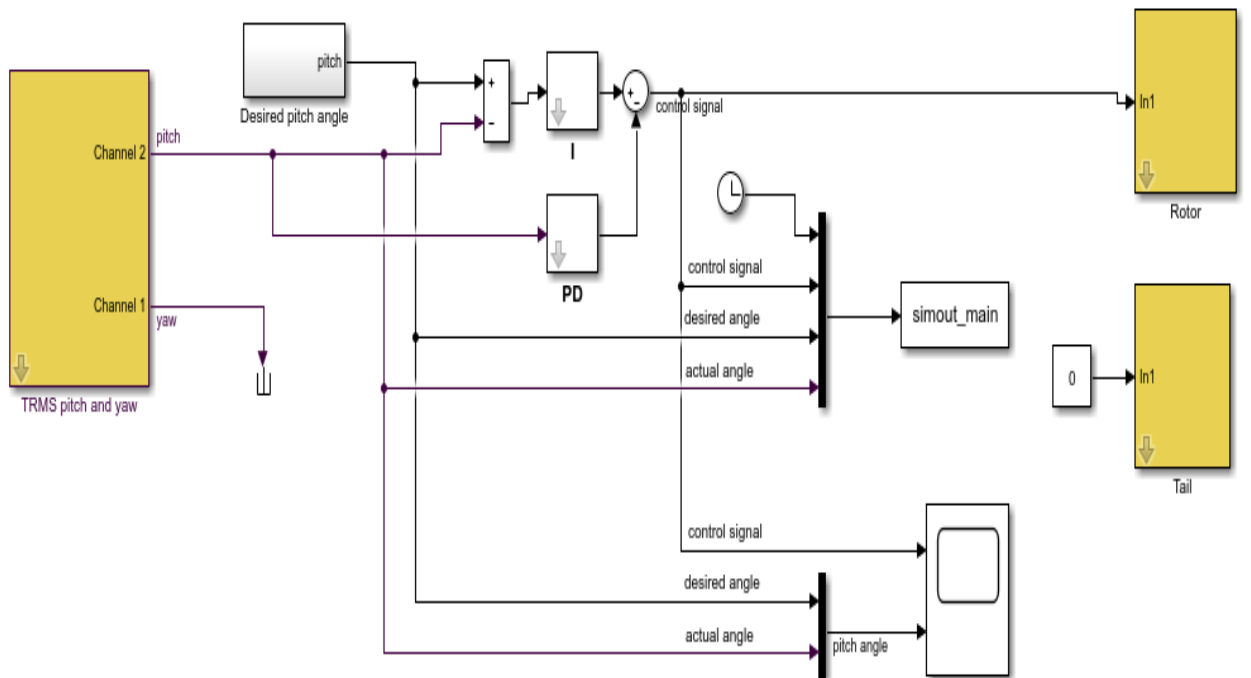


**Figure 4.6 Yaw angle control using FOI-PD**





### 4.3 IO-PID CONTROLLER

**Figure 4.7 Pitch angle control using IO-PID**

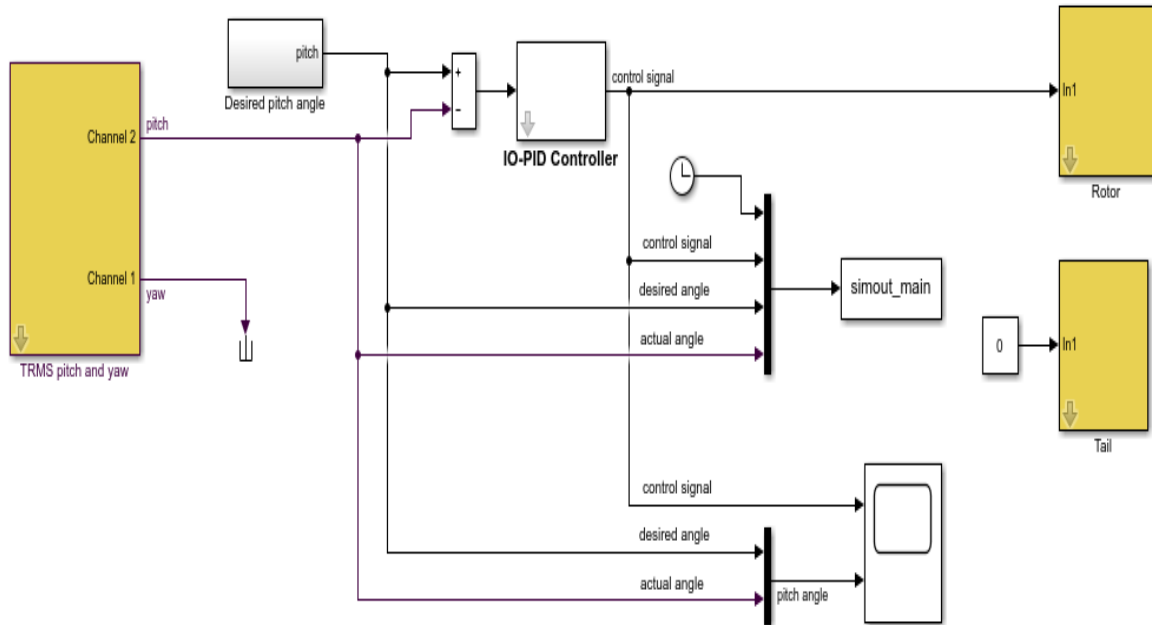
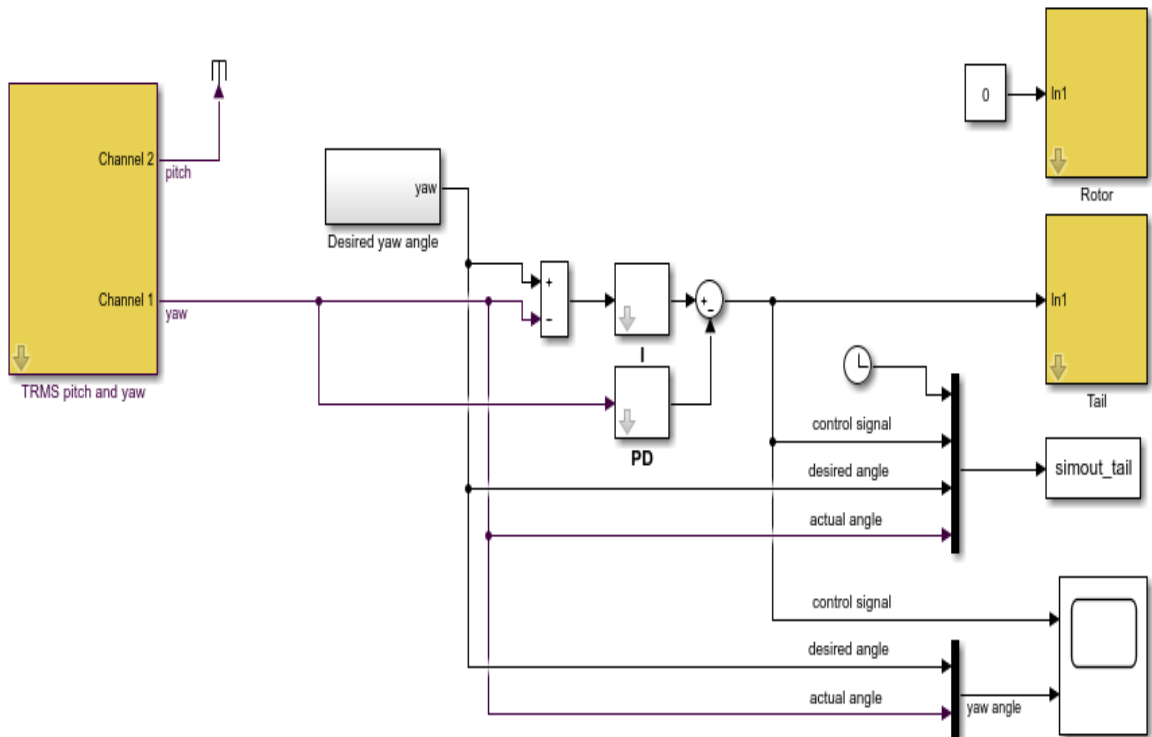


**Figure 4.8 Yaw angle control using IO-PID**



## 4.4 PROBLEM FORMULATION AND OBJECTIVE FUNCTION OPTIMIZATION

While designing the controller, the maximum percentage overshoot 5 % and settling time less than 10 seconds is considered to be a reasonably good design specification (although it varies from application to application). In the designing of controller for TRMS, the same design specifications are chosen i.e. Peak overshoot  $\leq 5\%$  and settling time  $t_s = 4/\zeta \omega_n \leq 10$  s. Using the optimal values of the design specifications, the values of  $\zeta$  and  $\omega_n$  are calculated and putting these values in the standard equation:  $s^2 + 2\zeta\omega_n s + \omega_n^2 = 0$

the dominants poles are calculated as:  $s_{12} = 0.4 \pm 0.4195i$

The characteristics equation of the system with FOI-PD controller is given by

$$1 + G_p(s) \left( \left( \frac{k_i}{s^\lambda} \right) + (k_p + k_d s^\beta) \right) = 0 \quad (113)$$

The transfer function model for the TRMS is given as:

$$G_{pitch}(s) = \tau_1 G_{11}(s) + \tau_2 G_{12}(s) \quad (114)$$

$$G_{yaw}(s) = \tau_1 G_{21}(s) + \tau_2 G_{22}(s) \quad (115)$$

Where  $\tau_1$  and  $\tau_2$  are the transfer function of the main rotor and tail rotor respectively already derived in Chapter two. Now, taking modulus of the characteristic polynomial which are calculated at dominant pole location, the following objective function has been obtained and are given by:

$$f_{pitch} = \min \left( \left| 1 + G_{pitch}(s) \left( k_{p1} + \frac{k_{i1}}{s^{\lambda 1}} + k_{d1} s^{\beta 1} \right) \right|_{s=s_1} \right) \quad (116)$$

$$f_{yaw} = \min \left( \left| 1 + G_{yaw}(s) \left( k_{p2} + \frac{k_{i2}}{s^{\lambda 2}} + k_{d2} s^{\beta 2} \right) \right|_{s=s_1} \right) \quad (117)$$

Minimizing the above objective function, we are trying to develop a set of controller parameters which gives ultimately satisfactory results for plant as well as controller. The objective function values after optimization is equivalent to zero in an ideal case. Indeed, numbers of cost functions are available in the literature and these functions can also be studied for optimization of the controller parameter. But this specific objective function was chosen for this research because of its simple implementation and flexibility.

#### 4.5 OPTIMIZATION OF OBJECTIVE FUNCTION

At first, Equations (111) and (112) were optimized individually using the function *fmincon* which is available in the MATLAB optimization toolbox for identifying the pitch and yaw angle control parameters of the IOPID controller by setting  $\lambda_1$ ,  $\beta_1$ ,  $\lambda_2$  and  $\beta_2 = 1$ . The range for the unknown parameters were carefully selected as the solution's optimality relies to a great extent on the range selected. At the initial stage of optimization, a wider solution space is considered and the space in the subsequent steps was reduced after the preliminary solution was obtained. Since the values of the simulation parameter do not guarantee success in real-time, choosing the range of controller parameters that will work both in simulation and in real-time is of primary importance. Table 4.1 provides the initial guess and the final range of parameter values of the controller to write the MATLAB code.

The values of “ $kp_1$ ,  $ki_1$ ,  $kd_1$ ,  $kp_2$ ,  $ki_2$  &  $kd_2$ ” have been found and are provided in Table 4.1 after optimizing the objective functions. To design the IOPID controller, the optimized set of controller parameter values has been used. In addition, the same set was considered to design the controller IOI-PD and FOI-PD. In the second stage, the values of fractional power of  $s$  relating to FOI-PD are obtained by optimizing the objective functions, keeping the controller gains the same as the IO-PID controller, reducing the number of Equations (111) and (112) unknowns from five to two. After the optimization of the following values of  $\lambda_1$ ,  $\beta_1$ ,  $\lambda_2$  and  $\beta_2$  have been found and provided in Table 4.2.

The optimized values of the controller parameters are either the lower or the upper parameter range. This behavior is expected because in nature the objective functions are convex and a global minimum was not found. It can definitely be considered an interesting problem of optimization to find the global optima. However, as our idea was to show the FOI-PD controller's superior behavior over the FO-PID and IO-PID controller in real time.

**Table 4.1 Range for the Controller parameters**

Objective	Parameters	Lower range	Upper range	Initial guess
Pitch angle control	$K_{p1}$	2.50	8.50	4.0
	$K_{i1}$	8.30	35.0	12.0
	$K_{d1}$	18.30	25.0	20.0
Yaw angle control	$K_{p2}$	5.0	17.0	15.0
	$K_{i2}$	17.50	25.0	20.0
	$K_{d2}$	30	35.0	32.0

**Table 4.2 Range for the Controller parameters**

Objective	Controller Parameter	Lower range	Upper range	Initial guess
Pitch angle control	$\lambda_1$	0.875	1.0	0.90
	$\beta_1$	0.925	1.0	0.95
Yaw angle control	$\lambda_2$	0.915	1.0	0.95
	$\beta_2$	0.925	1.0	0.95

**Table 4.3 Optimized values for FO-PID Controller parameter**

Objective	Parameters	Optimized value
Pitch angle control	$K_{p1}$	7.46
	$K_{i1}$	34.31
	$K_{d1}$	15.30
Yaw angle control	$K_{p2}$	7.66
	$K_{i2}$	3.47
	$K_{d2}$	2.84

**Table 4.4 Optimized values for IO-PID Controller parameter**

<b>Objective</b>	<b>Parameters</b>	<b>Optimized value</b>
Pitch angle control	$K_{p1}$	5.5
	$K_{i1}$	8.3
	$K_{d1}$	18.3
Yaw angle control	$K_{p2}$	17
	$K_{i2}$	17.5
	$K_{d2}$	30

**Table 4.5 Optimized values for Controller parameter**

<b>Objective</b>	<b>Parameters</b>	<b>Optimized value</b>
Pitch angle control	$\lambda_1$	0.875
	$\beta_1$	0.925
Yaw angle control	$\lambda_2$	0.915
	$\beta_2$	0.925

## CHAPTER 5

### RESULTS AND DISCUSSIONS

FO-PID'S & IO-PID has been designed separately for controlling the vertical and horizontal movement i.e. pitch rotor and yaw rotor in decoupled mode. Here the real time experiments are performed for 1-DOF plane.

The real time response of non-linear model of TRMS for horizontal as well as vertical are shown in figures (5.1-5.12). The pitch and yaw angles are controlled separately by FO-PID, & also FOI-PD and IO-PID controllers respectively. The TRMS model is operated near its equilibrium points (origin). Average of three different sinusoidal waves of duration 100 seconds and having amplitude between 0 to 1 are chosen as reference signal for horizontal and vertical movement control. Average of vertical reference signal is found as 0.42 radians whereas horizontal reference signal has average of 0.57 radians.

It is concluded that both FOI-PD and FO-PID gives satisfactory response than IO-PID controller by tracking the desired pitch as well as yaw angle respectively. In case of FOI-PD controller the response time for stabilization is much lesser than FO-PID and IO-PID.

It is observed that IO-PID response has larger spikes and it takes more time to stabilize than FO-PID and because of the derivative kick phenomena occurring in IO-PID controller which can be avoided in the case of FOI-PD and FO-PID. It is observed that the energy of the control signal is minimum in case of the FOI-PD controller as compared to the FO-PID and IO-PID controller for both pitch and yaw angle control.

## 5.1 Real time response of (FO-PID)

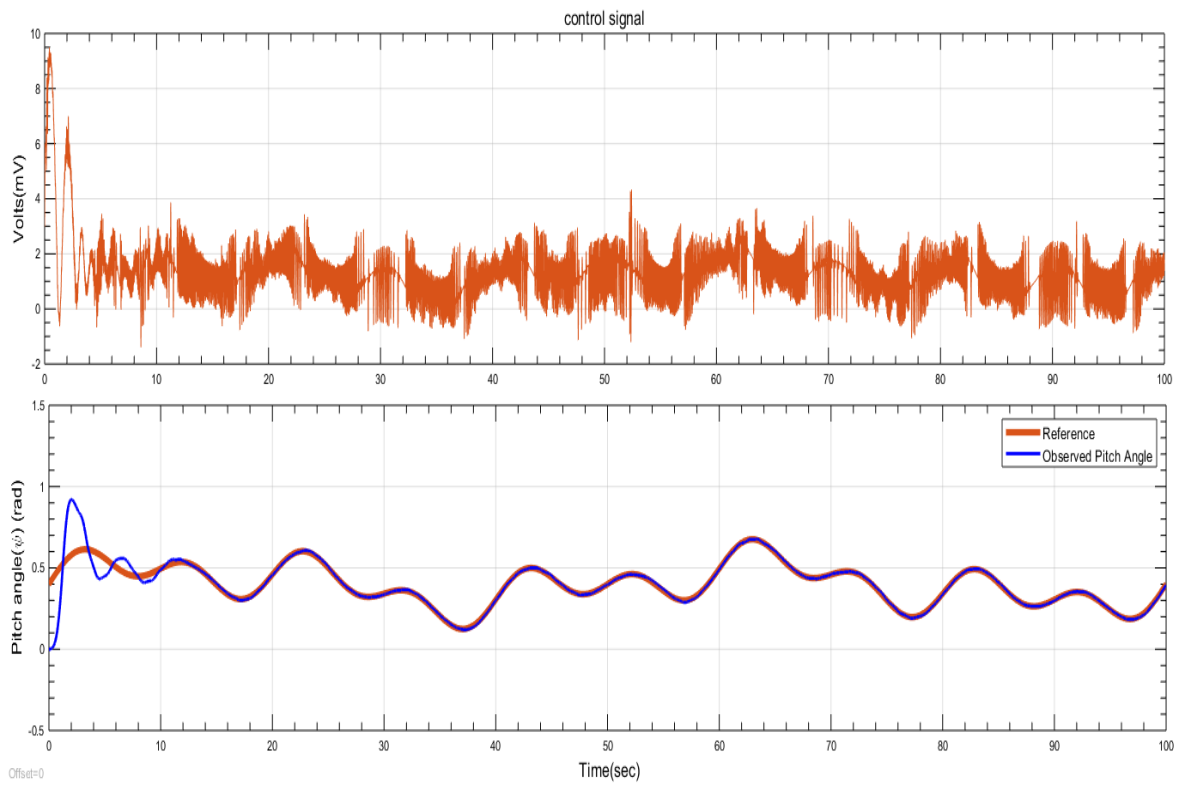


**Figure 5.1 FOPID Pitch Angle Plot (without disturbance)**

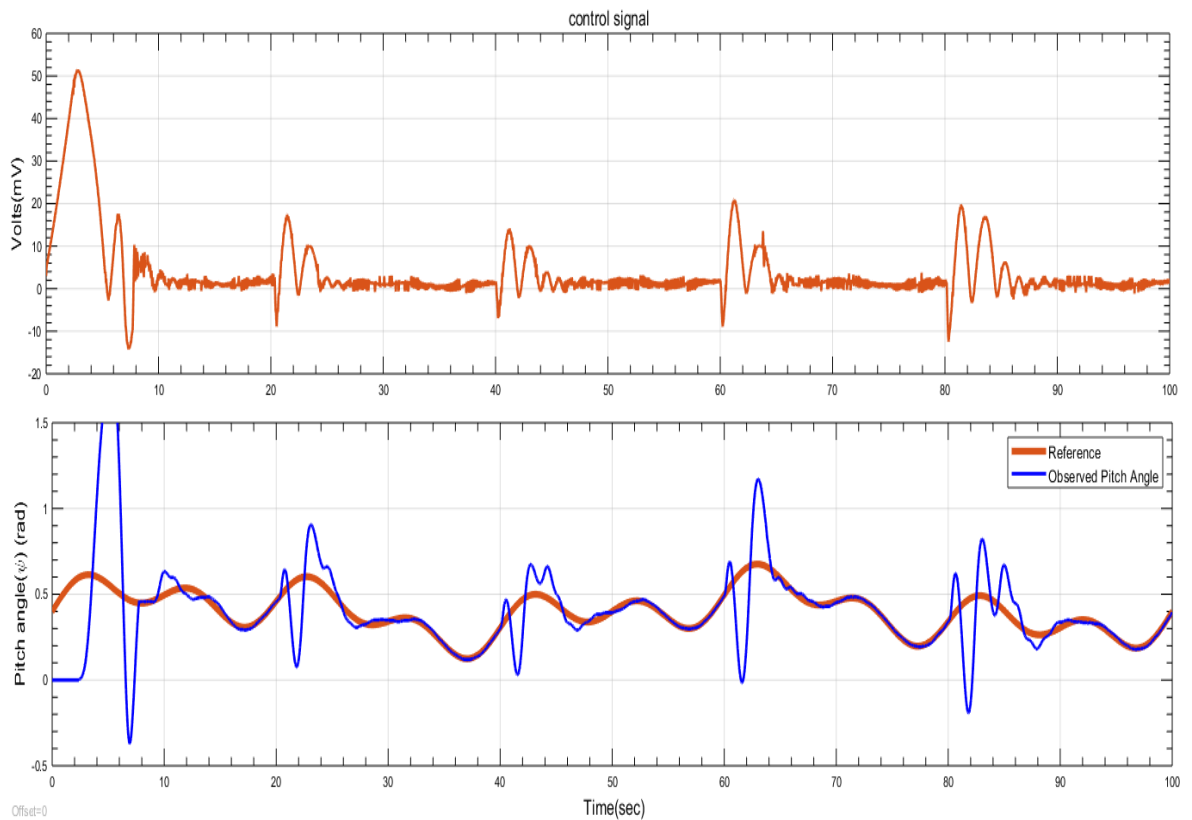


**Figure 5.2 FOPID Pitch Angle Plot (with disturbance)**

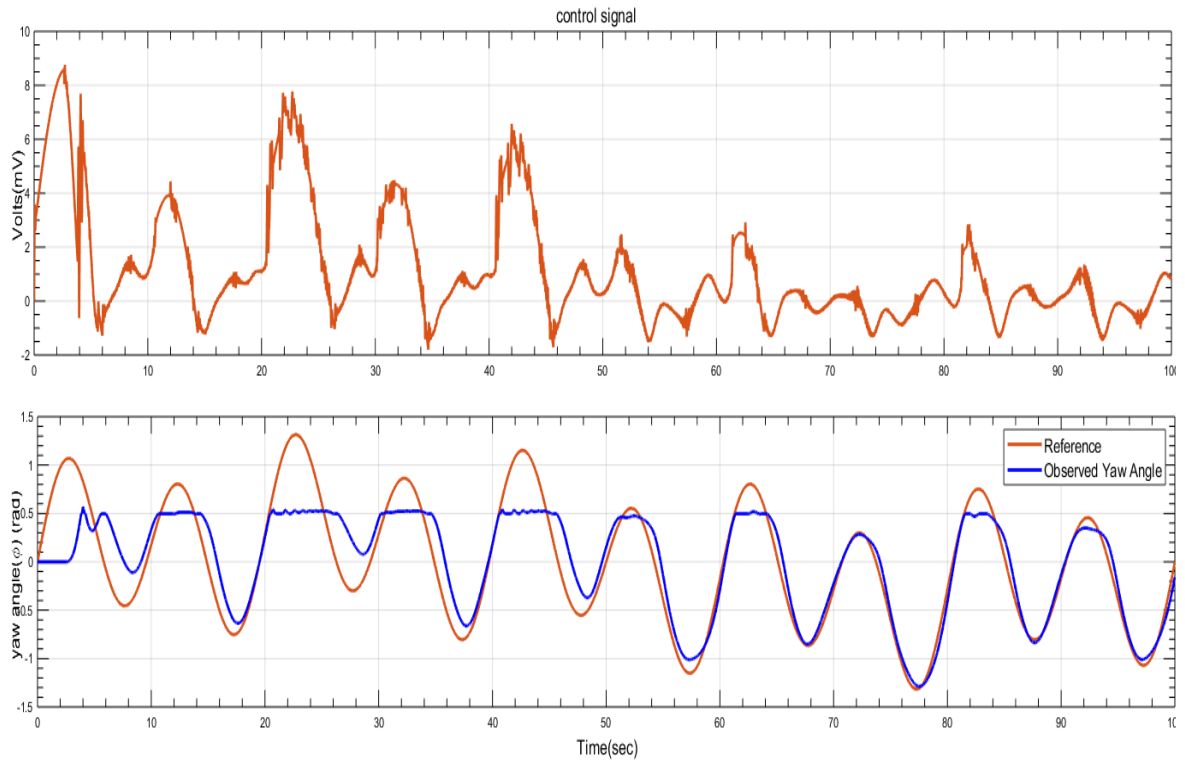


**Figure 5.3 Yaw Angle Control (without disturbance)**

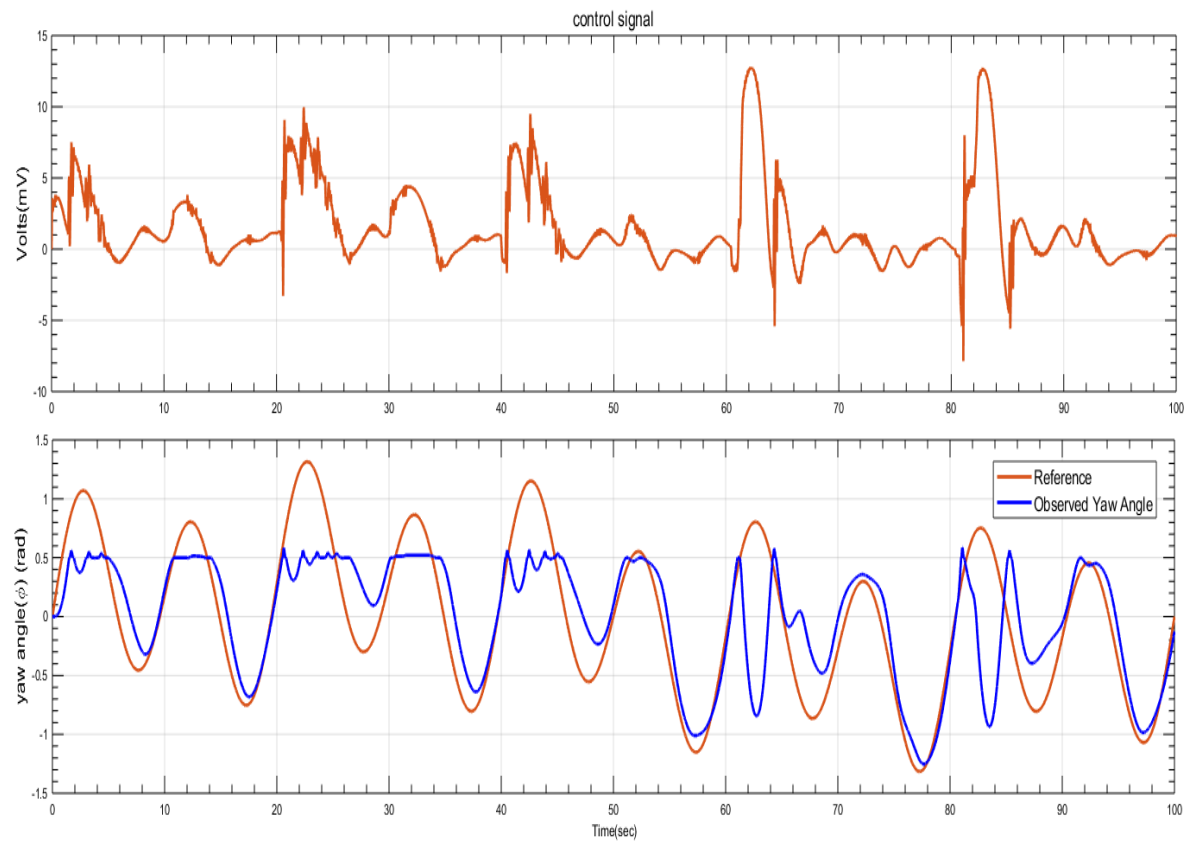


**Figure 5.4 Yaw Angle Control (with disturbance)**



## 5.2 Real time Response (FOI-PD)

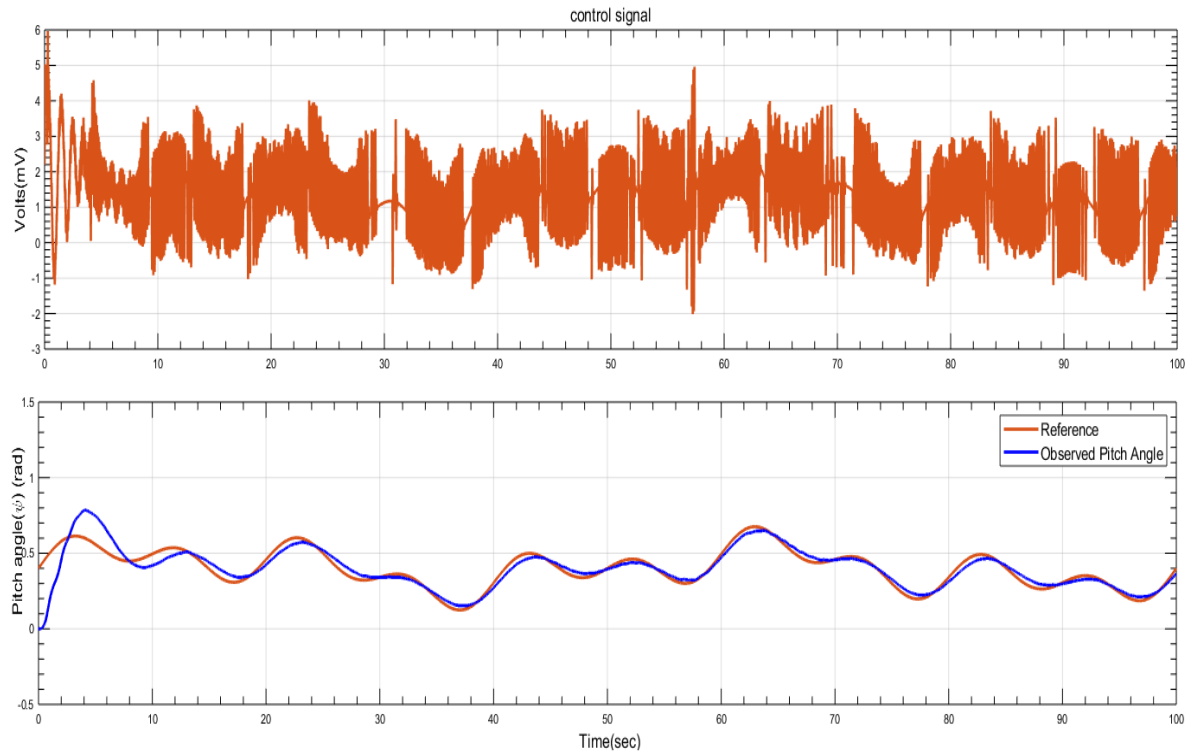


**Figure 5.5 FOI-PD Pitch Angle Plot (without disturbance)**

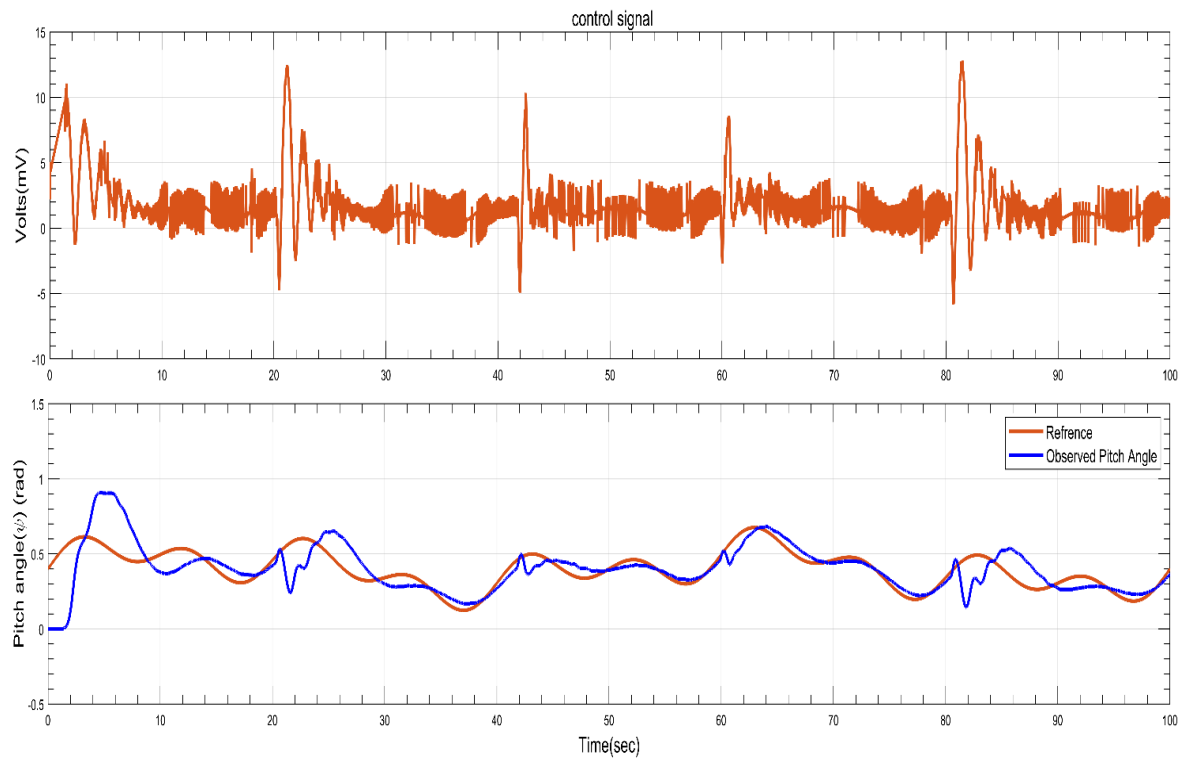


**Figure 5.6 FOI-PD Pitch Angle Plot (with disturbance)**

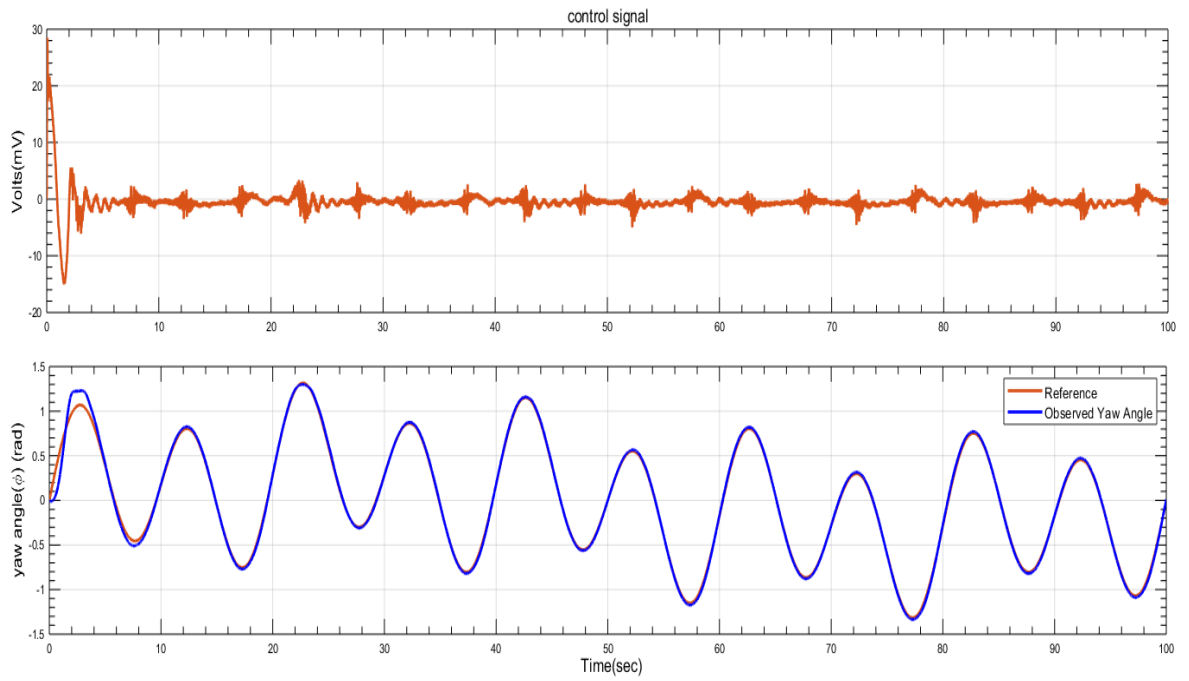


**Figure 5.7 FOI-PD Yaw Angle Plot (without disturbance)**

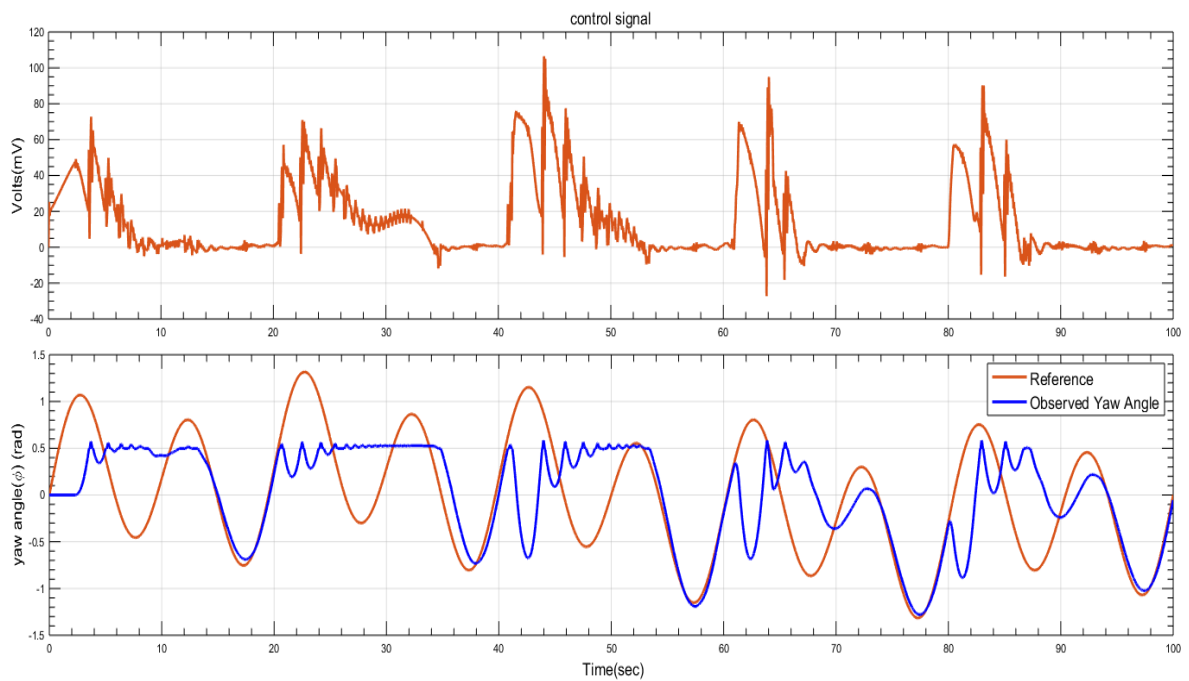


**Figure 5.8 FOI-PD Yaw Angle Plot (with disturbance)**

**Figure 5.8 FOI-PD Yaw Angle Plot (with disturbance)**

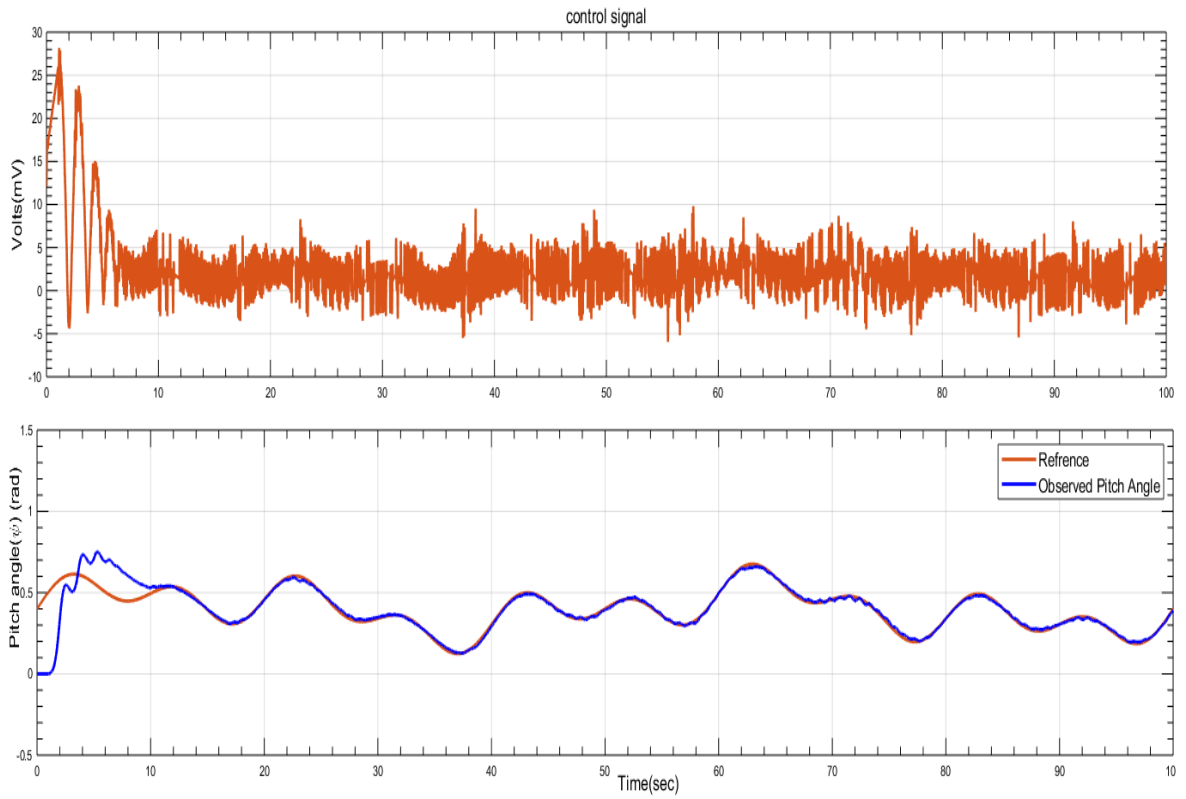


**Figure 5.9 IO-PID Pitch Angle Plot (without disturbance)**

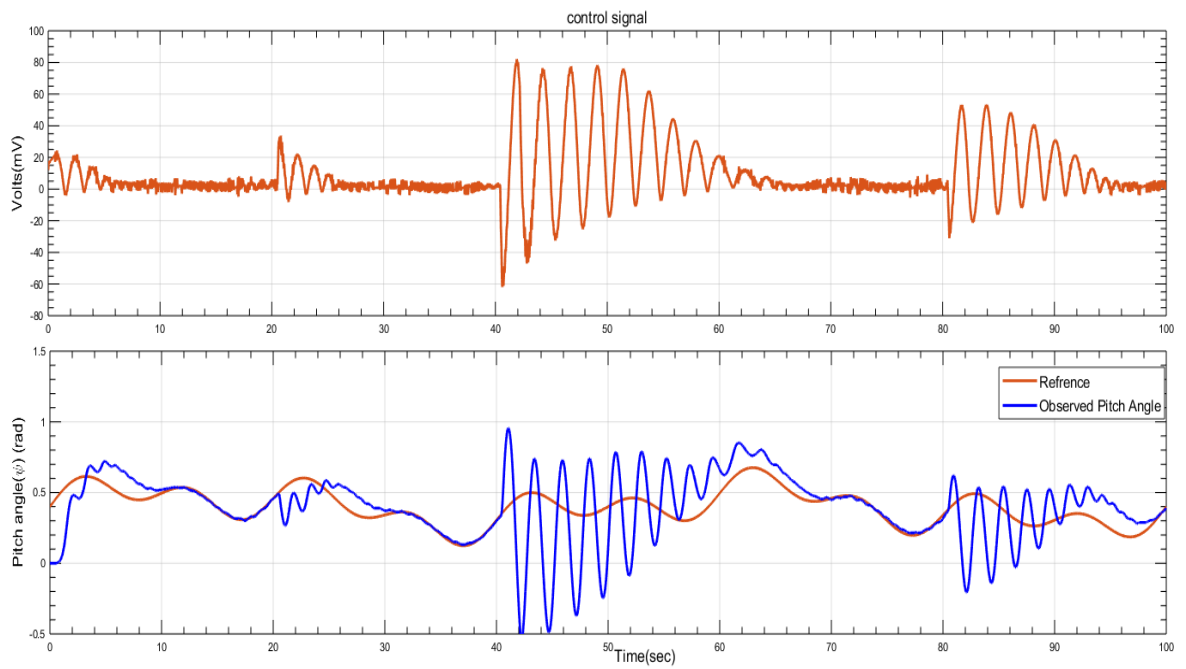


**Figure 5.10 IO-PID Pitch Angle Plot (with disturbance)**

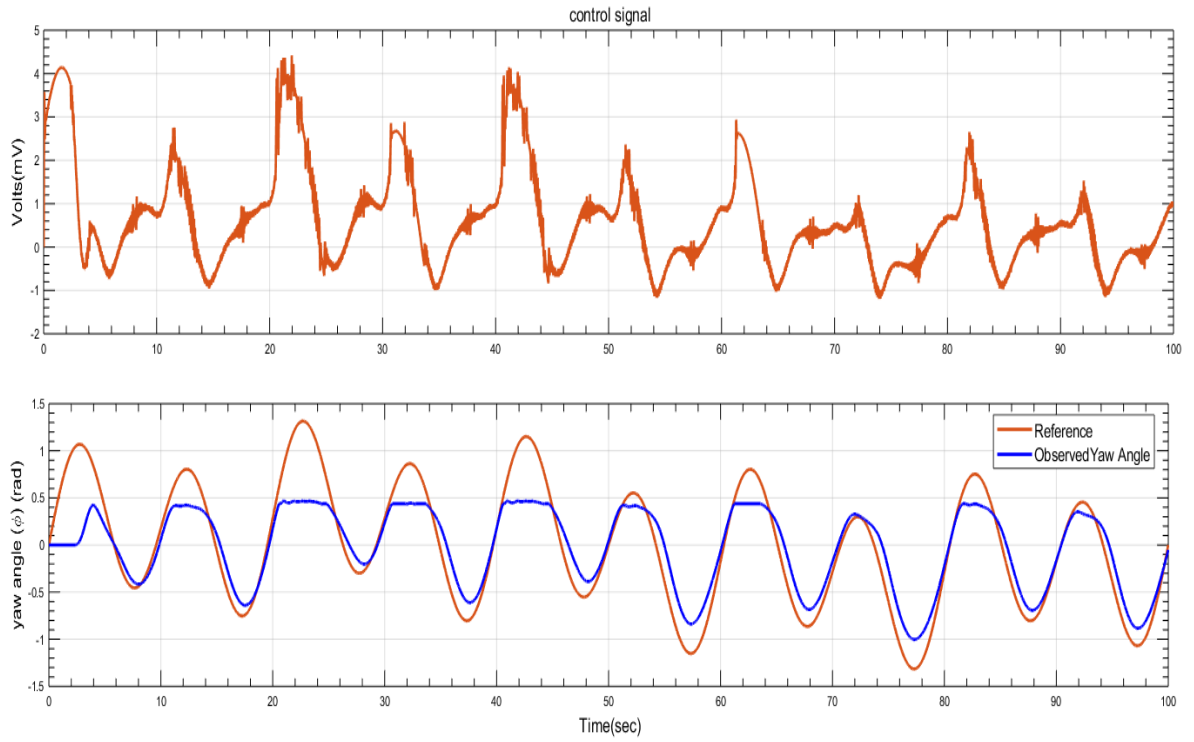


**Figure 5.11 IO-PID Yaw Angle Plot (without disturbance)**

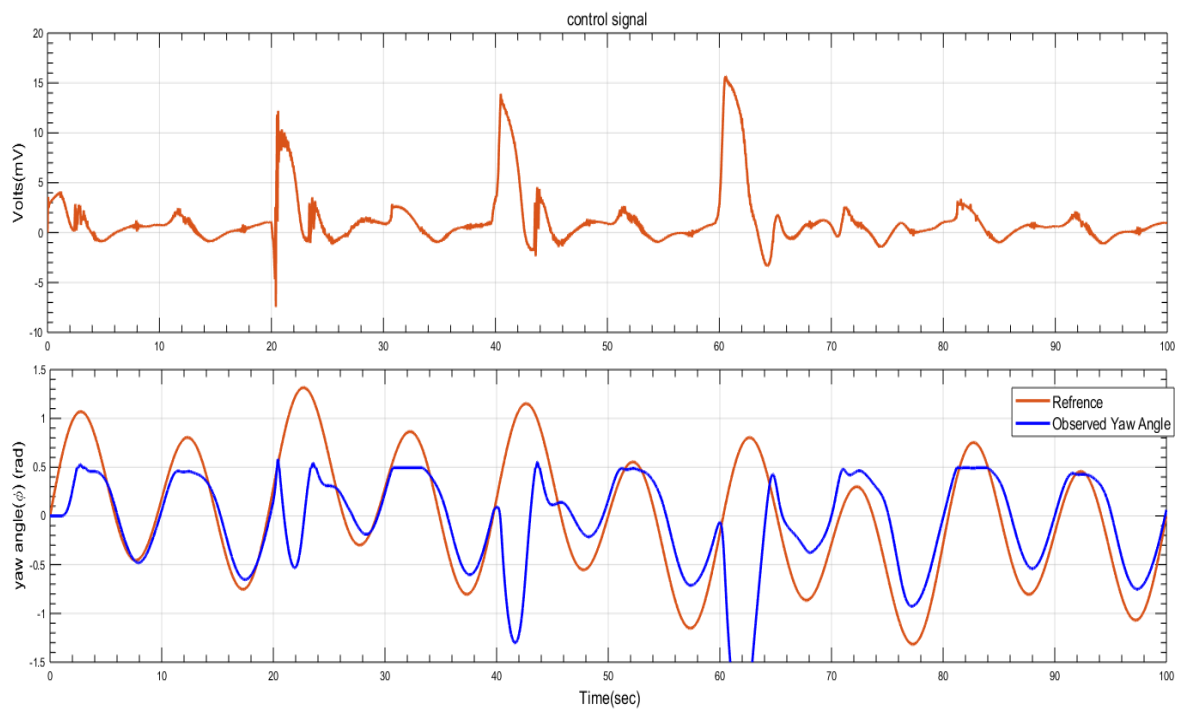


**Figure 5.12 IO-PID Yaw Angle Plot (with disturbance)**

## 5.4 COMPARATIVE ANALYSIS OF FO-PID, FOI-PD & IO-PID CONTROLLERS

The following real time response of controllers are obtained for random disturbances given at different time instants (20<sup>th</sup>, 40<sup>th</sup>, 60<sup>th</sup> and 80<sup>th</sup> seconds) for controlling of pitch and yaw angle respectively. The stabilization time for various controllers has been noted and from that a comparative analysis on the performance of above controllers is concluded in the next section.

	FOI-PD			FOPID			IO-PID		
	Disturbance given at (sec)	Settled at (sec)	Stabilizing time (sec)	Disturbance given at (sec)	Settled at (sec)	Stabilizing time (sec)	Disturbance given at (sec)	Settled at (sec)	Stabilizing time (sec)
P I T C H	20th	29th	9	20th	30th	10	20th	32th	12
	40th	50th	10	40th	52th	12	40th	70th	30
	60th	64th	4	60th	68th	8	60th	70th	10
	80th	89th	9	80th	94th	14	80th	99th	19
Y A W	20th	34th	14	20th	35th	15	20th	35th	15
	40th	54th	14	40th	53th	13	40th	54th	14
	60th	70th	10	60th	70th	10	60th	74th	14
	80th	90th	10	80th	93th	13	80th	94th	14

From the above table it is observed that time taken to stabilize the TRMS pitch and yaw angle control for tracking of desired reference signal after giving disturbances is least in FOI-PD followed by FO-PID and then IO-PID controllers.

## CHAPTER 6

### CONCLUSION

In this thesis, modelling and controlling of Twin rotor MIMO system has been presented. Three different controllers are designed namely (i) FO-PID (ii) FOI-PD (iii) IO-PID for controlling of vertical as well as horizontal movement and implemented in the real time for Twin Rotor MIMO System by optimizing the objective functions using the function *fmincon*.

For real time experimentation we introduce random disturbances to the TRMS system at different time instances (20<sup>th</sup>, 40<sup>th</sup>, 60<sup>th</sup> and 80<sup>th</sup> seconds) and the performance of the controllers has been compared. It is observed that the control signal gets improved as we moves from the FO-PID to FOI-PD and integer order to fractional order.

From the real time implementation of above three controllers on Twin rotor MIMO system shows that FOI-PD controller gives best performance for stabilizing and tracking of desired pitch and yaw angle when the random disturbance is given to TRMS followed by FO-PID and then IO-PID.

#### 6.2 FUTURE SCOPE

As a future research scope, MIMO Fractional Order controller can be designed for controlling the unstable nonlinear systems such as TRMS and advanced control strategies such as adaptive control scheme can also be explored to produce smooth control signal. In addition, in order to improve device efficiency and accurate trajectory tracking, this particular method of developing the FOI-PD controller may be expanded to other plant categories used in UAV<sup>s</sup> applications in future.

## REFERENCES

- [1] Feedback Instruments, “Twin Rotor Mimo System,” 2016.
- [2] N. Almtireen, H. Elmoaqet, and M. Ryalat, “Linearized Modelling and Control for a Twin Rotor System,” *Automatic Control and Computer Sciences*, vol. 52, no. 6, pp. 539–551, 2019.
- [3] P. Wen and Y. Li, “Twin rotor system modeling, de-coupling and optimal control,” in *IEEE International Conference on Mechatronics and Automation*, 2011, pp. 1839–1842.
- [4] S. Ramalakshmil and S. Manoharan, “Non-linear Modeling and PID Control of Twin Rotor MIMO System,” in *IEEE International Conference on Advanced Communication Control and Computing Technologies (ICACCCT)*, 2012, no. 978, pp. 366–369.
- [5] I. Z. M. Darus, F. M. Aldebrez, and M. O. Tokhi, “Parametric modelling of a twin rotor system using genetic algorithms,” in *First International Symposium on Control, Communications and Signal Processing, 2004.*, 2004, pp. 115–118.
- [6] S. Miah, M. R. Kafi, and H. Chaoui, “Generalized Cascaded Control Technology for a Twin-Rotor MIMO System with State Estimation,” *Journal of Control, Automation and Electrical Systems*, vol. 30, no. 2, pp. 170–180, 2019.
- [7] M. S. and V. K. Sudarshan K. Valluru Madhusudan Singh, “Experimental Validation of PID and LQR Control Techniques for Stabilization of Cart Inverted Pendulum System,” in *3rd IEEE International conference on Recent Trends in Electronics, Information and communication Technology*, 2018, pp. 708–712.
- [8] D. Sain, S. K. Swain, A. Saha, S. K. Mishra, and S. Chakraborty, “Real-Time Performance Analysis of FOI-PD Controller for Twin Rotor MIMO System,” *IETE Technical Review*, pp. 1–22, 2018.
- [9] T. Dang Huu and I. B. Ismail, “Modelling of twin rotor MIMO system,” in *2016 2nd IEEE International Symposium on Robotics and Manufacturing Automation (ROMA)*, Ipoh, Malaysia, 2016, pp. 1–6.
- [10] S. M. Ahmad, A. J. Chipperfield, and O. Tokhi, “Dynamic modeling and optimal control of a twin rotor MIMO system,” *Proceedings of the IEEE 2000 National Aerospace and Electronics Conference. NAECON 2000. Engineering Tomorrow* (Cat. No.00CH37093), Dayton, OH, 2000, pp.391–8.
- [11] J. K. Pradhan and A. Ghosh, “Design and implementation of decoupled compensation for a twin rotor multiple-input and multiple-output system,” *IET Control Theory*

- [12] P. Chalupa, J. Prikryl, and J. Novak, "Modelling of twin rotor MIMO system," *Procedia Eng.*, Vol. 100, pp. 249–58, 2015.
- [13] S. Saxena and Y. V. Hote, "Design and validation of fractional-order control scheme for DC servomotor validation model control approach," *IETE Tech. Rev.*, 2017.
- [14] M. R. Faieghi and A. Nemati, "On fractional-order PID design," in *Applications of MATLAB in Science and Engineering*, T. Michalowski Ed. Rijeka: Intech, 2011, pp. 273–92.